

Hydrogeomorphic Effects of Explosive Volcanic Eruptions on Drainage Basins*

Thomas C. Pierson and Jon J. Major

Volcano Science Center, Cascades Volcano Observatory, US Geological Survey, Vancouver, Washington 98683; email: tpierson@usgs.gov, jjmajor@usgs.gov

Annu. Rev. Earth Planet. Sci. 2014. 42:469–507

The *Annual Review of Earth and Planetary Sciences* is online at earth.annualreviews.org

This article's doi:

[10.1146/annurev-earth-060313-054913](https://doi.org/10.1146/annurev-earth-060313-054913)

*This is a work of the US Government and is not subject to copyright protection in the United States.

Keywords

explosive volcanic eruptions, runoff, volcanoclastic sedimentation, volcanic drainage basins, geomorphic recovery, sediment yield

Abstract

Explosive eruptions can severely disturb landscapes downwind or downstream of volcanoes by damaging vegetation and depositing large volumes of erodible fragmental material. As a result, fluxes of water and sediment in affected drainage basins can increase dramatically. System-disturbing processes associated with explosive eruptions include tephra fall, pyroclastic density currents, debris avalanches, and lahars—processes that have greater impacts on water and sediment discharges than lava-flow emplacement. Geomorphic responses to such disturbances can extend far downstream, persist for decades, and be hazardous. The severity of disturbances to a drainage basin is a function of the specific volcanic process acting, as well as distance from the volcano and magnitude of the eruption. Postdisturbance unit-area sediment yields are among the world's highest; such yields commonly result in abundant redeposition of sand and gravel in distal river reaches, which causes severe channel aggradation and instability. Response to volcanic disturbance can result in socioeconomic consequences more damaging than the direct impacts of the eruption itself.

INTRODUCTION

Explosive volcanic eruptions are geologically discrete events that provide awesome displays of nature's power. That power, often devastating and sometimes deadly, can force landscape changes (disturbances) that have widespread and long-lasting repercussions on the interrelated hydrologic and geomorphic (hydrogeomorphic) components of the affected landscapes. Hydrogeomorphic responses to volcanic disturbances can persist and prove hazardous long after an eruption has ceased. Indeed, the hydrogeomorphic responses to landscape disturbances caused by explosive eruptions can have greater socioeconomic consequences than the direct impacts of the eruptions themselves (e.g., Willingham 2005).

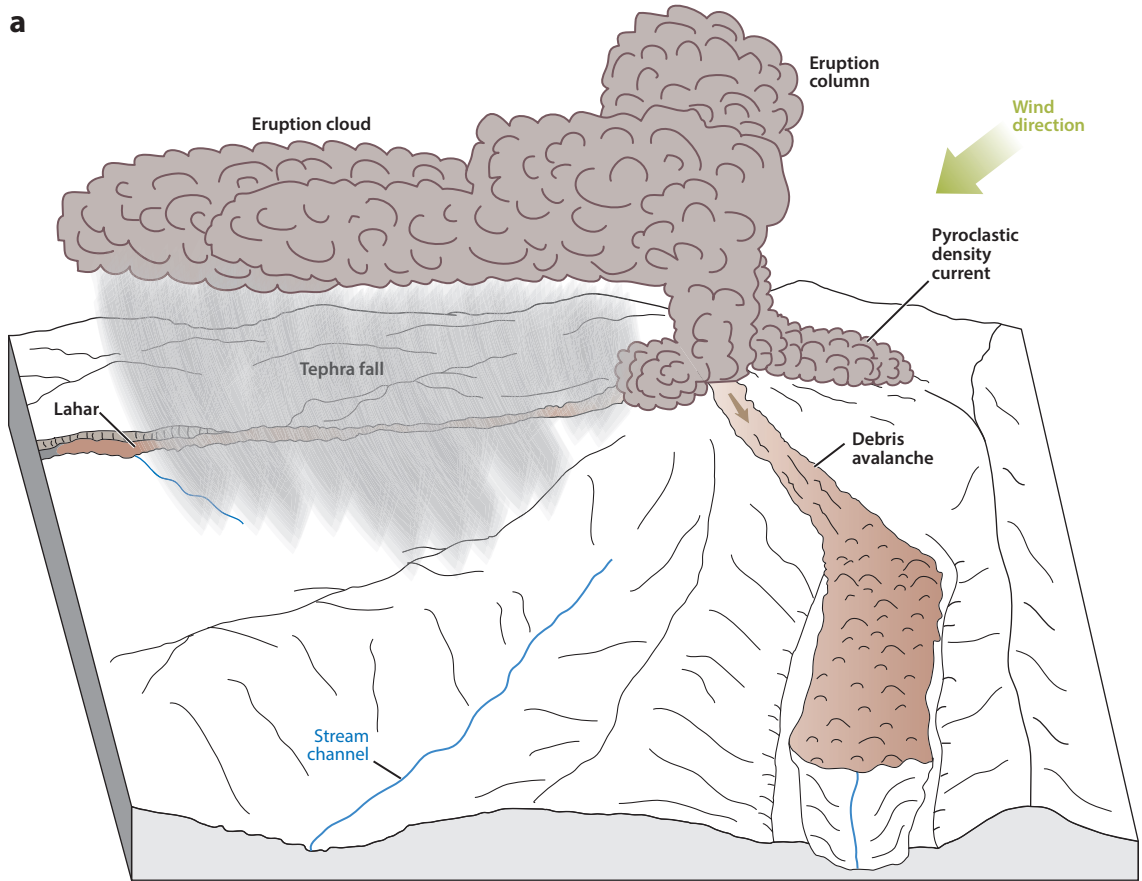
Explosive eruptions can disturb landscapes in a variety of ways (**Figure 1**). They can produce large quantities of relatively fine-grained tephra—particles of volcanic rock—and disperse it over very large areas ($>10^6$ km²), where it can engender a host of physical, chemical, and biological effects (Ayris & Delmelle 2012). Tephra is composed primarily of pyroclastic (primary volcanoclastic) particles explosively ejected during eruptions and deposited by the fallback of ejected particles (tephra fall) or by gravity-driven or explosion-driven dry flows of solid particles, gases, and air (pyroclastic density currents), including flows generated by collapsing lava domes and lava flows (block-and-ash flows). In addition, explosive eruptions commonly trigger additional processes that produce and deposit large quantities of volcanic rock particles generally not defined as tephra: debris avalanches, which are dry or unsaturated granular flows formed from gravitational collapses of destabilized sectors of volcanic edifices; and lahars, which are saturated flows of rock particles and water formed from entrainment of rock particles by large water discharges or from the transformation of debris avalanches (see sidebar, Volcanic Process Terminology). Explosive eruptions producing large volumes of tephra and other fragmental rock debris are common at volcanoes of intermediate and silicic composition in volcanic arcs.

Explosive eruptions can affect individual or collective units of landscape known as drainage basins (also termed watersheds or catchments). These basins can be viewed, over a range of scales, as fluvial systems, which are defined by surface-water streams and the terrain that spatially confines them; the sediment that is eroded and transported by them; and the energy inputs to and boundary conditions of the basin, which drive and modulate the dynamic interactions among water, sediment, and geomorphology (Piégay & Schumm 2003). Fluvial systems are self-regulating and typically, in the absence of large disturbances, tend toward a stable (or metastable) equilibrium or steady-state condition that is dependent on spatial scales and timescales and is defined by consistency in mass flux and surface morphology (Thorn & Welford 1994, Phillips 2009, Wu et al. 2012). This means that landforms self-adjust through negative feedback mechanisms to be more or less in balance with average fluxes of water, sediment, and energy over given timescales and spatial scales, although no single pathway to equilibrium or single equilibrium state is implied. Explosive eruptions disrupt fluvial-system equilibrium by emplacing large volumes of volcanoclastic particles on the landscape; emplacement of these particles drastically alters boundary conditions and increases mass flux (water and sediment) in the affected drainage basin. Geomorphic responses to increased water and sediment fluxes commonly include increased magnitude, frequency, and spatial extent of seasonal

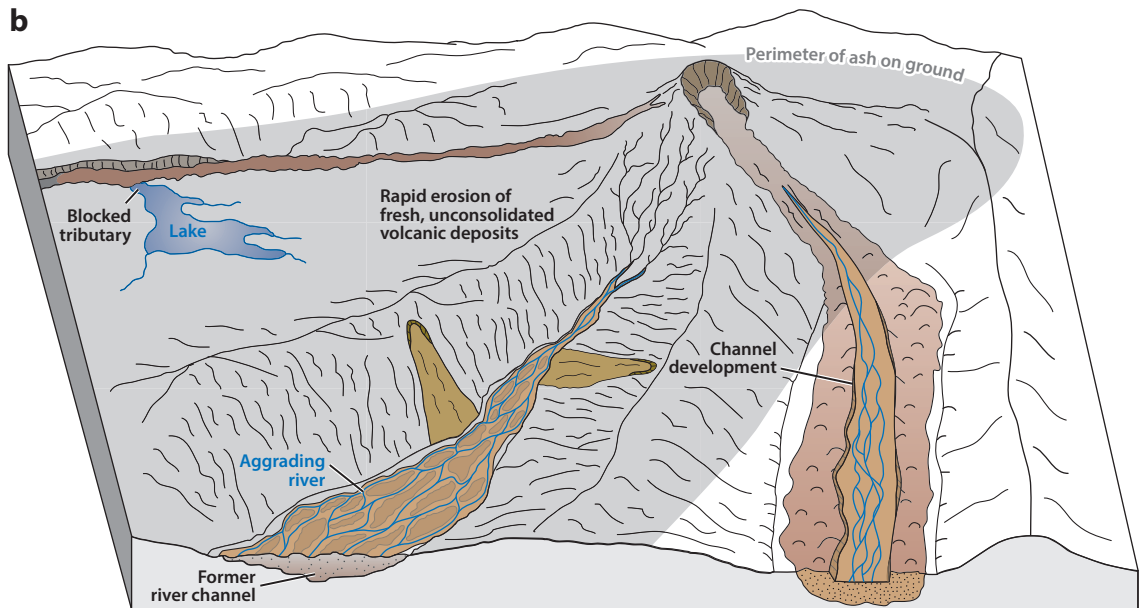
Figure 1

Diagram illustrating explosive eruption processes and subsequent landscape responses. (a) Volcanic processes from or related to an explosive eruption, including tephra fall, pyroclastic density currents, a debris avalanche, and a lahar. (b) Landscape changes and responses to disturbances caused by the eruption processes shown in panel a include rapid erosion of fresh tephra by rilling and landsliding, erosion of channel fill and development of new channel networks, channel aggradation and formation of braided channel patterns, and impoundment of channel-margin lakes.

a



b



VOLCANIC PROCESS TERMINOLOGY

Tephra: Collective term for particles of volcanic rock (of any size, shape, or composition) ejected in an explosive volcanic eruption. Formation mechanisms include fragmentation of magma during eruption by explosive exsolution of magmatic gas, and fragmentation of volcanic rock by steam-driven explosions occurring when hot magma interacts with groundwater (White & Houghton 2006, Cashman & Sparks 2013). Tephra particles are also termed pyroclastic or primary volcanoclastic particles. Once the particles in tephra deposits are remobilized by geomorphic processes (gravitational sliding or flow, or entrainment by flowing water, ice, or air), they are reclassified as secondary volcanoclastic deposits or simply volcanoclastic sediment (White & Houghton 2006).

Terminology for pyroclastic particles includes the following:

- **Ash:** pyroclastic particles <2 mm in diameter
- **Lapilli:** pyroclastic particles 2–64 mm in diameter
- **Blocks or bombs:** pyroclastic particles >64 mm in diameter (bombs have fluidal morphology)

Sizes of secondary volcanoclastic particles are described using standard sedimentological size terminology (i.e., clay, silt, sand, pebbles, cobbles, and boulders; Folk 1980).

Tephra fall: Rain of pyroclastic rock particles to the ground following ejection into the air by explosive eruptions (Houghton et al. 2000, Bonadonna & Costa 2013). Aerosol droplets of acid (HCl, H₂SO₄, HF) commonly adhere to ash particles (Mills 2000).

Pyroclastic density current (PDC): Rapid flow of a dry mixture of hot solid particles, gases, and air, which can range in character from a dense, ground-hugging, granular flow (pyroclastic flow) to a turbulent, low-density dust cloud of mostly fine ash and superheated air (pyroclastic surge). A single PDC commonly involves both flow types due to gravitational segregation. Flows are generally gravity driven but may be accelerated initially by impulsive forces of volcanic explosions. PDCs form during sustained, high-energy, explosive eruptions; when relatively low-energy explosive eruptions fountain or bubble over from a vent; and when portions of hot lava domes or lava flows collapse, disintegrate, and commence avalanching downslope (Wilson & Houghton 2000; Branney & Kokelaar 2002; Belousov et al. 2007, 2011; Roche et al. 2013). Flows from collapsed lava domes and lava flows are commonly known as block-and-ash flows.

Debris avalanche: Rapid granular flow of an unsaturated or partially saturated mixture of volcanic rock particles (\pm ice) and water, initiated by the gravitational collapse and disintegration of part of a volcanic edifice (McGuire 1996, Siebert 2002). Debris avalanches commonly occur when magma intrudes high into, and destabilizes, a volcanic edifice, but they can also be triggered during noneruptive periods by earthquakes, ground deformation beneath volcanoes, edifice overloading and oversteepening as volcanoes grow, peripheral erosion, extended heavy rainfall, changes in sea level, pressurization by hydrothermal fluids, and gradual mechanical weakening of rock by hydrothermal alteration. Although debris avalanches commonly occur in association with eruptions, they also can occur during periods when a volcano is dormant.

Lahar: Rapid granular flow of a fully saturated mixture of volcanic rock particles (\pm ice) and water (Vallance 2000, 2005). Major initiation mechanisms, which occur during both eruptions and noneruption periods, include direct transformation of debris avalanches, rapid melting of snow and ice during eruptions, outbreaks of impounded lakes, and rainfall on fresh tephra deposits. A lahar that has >50% solids by volume is termed a debris flow; one that has roughly 10–50% solids by volume is termed a hyperconcentrated flow (Pierson 2005). Flow type can evolve with time and distance along a flow path as sediment is entrained or deposited, and both types are more erosive and transport and deposit much greater volumes of sediment than muddy water floods, which typically are <10% solids by volume.

floods; major shifts in river channel morphology, position, and bed elevation; drastically increased sediment yields; and generation of significant volcano-hydrologic hazards that can continue long after eruptive activity has ceased. Although mafic eruptions that produce widespread lava flows (e.g., Hawaii or the central Oregon Cascades, United States) can also disrupt basin hydrology and sediment transport, the hydrologic and geomorphic responses to lava-flow-producing eruptions are generally less consequential than are those to explosive eruptions (Jefferson et al. 2010). We therefore focus on responses to explosive eruptions.

Geomorphic response to a discrete volcanic disturbance typically involves a reaction time, a destabilization time, and a relaxation time (**Figure 2**). The rate of change of hydrogeomorphic adjustments occurs rapidly immediately after disturbance and then more gradually with time to become asymptotic with the new equilibrium state (Graf 1977, Wu et al. 2012). The combined disequilibrium period (reaction + relaxation times) in volcanically disturbed drainage basins is termed the syneruption period (Smith 1991). Periods of equilibrium following hydrologic and geomorphic adjustment to volcanic disturbance are termed intereruption periods. Typically, syneruption periods are short relative to intereruption periods at a given volcano or volcanic region (Smith 1991). During intereruption periods, average water and sediment fluxes (measured as streamflow and sediment yield) in previously disturbed drainage basins are similar to those of nearby basins that have never been, or have seldom been, disturbed by volcanic eruptions. In the Cascade Range of the Pacific Northwest, for example, basins seldom affected by eruptions are characterized by dense forest vegetation, steep slopes, and permeable organic soils. Their basin hydrology reflects low- to moderate-intensity seasonal rainfall, primarily subsurface runoff pathways, low direct runoff ratios (ratio of surface runoff to total precipitation), vigorous evapotranspiration, and moderately low sediment yields (e.g., Jones 2000, Roering et al. 2010, Czuba et al. 2011).

The effects of explosive eruptions on landscapes near volcanoes have been recognized since at least the early 1900s (e.g., Anderson & Flett 1903), but the magnitude of their geological and social significance has become more acutely appreciated over the past few decades as a result of studies following a few particularly significant and well-studied eruptions: Taupo, New Zealand, 1.8 ka; Irazú, Costa Rica, 1963–1965; Sakurajima, Japan, 1955–present; Usu, Japan, 1977–1978; Unzen, Japan, 1991–1995; Miyakejima, Japan, 2000; Mount St. Helens, United States, 1980; Nevado del Ruiz, Colombia, 1985; Mount Pinatubo, Philippines, 1991; Mount Merapi, Indonesia, 1994 and 2010; Montserrat, West Indies, 1995–present; and Chaitén, Chile, 2008–2009. A recent comprehensive review of the evolution of our understanding of volcanoclastic processes and deposits is given by Manville et al. (2009a). Our review focuses on (a) the effects of emplacement of volcanoclastic deposits on surface-water hydrology and sedimentation in drainage basins on or near volcanoes and (b) geomorphic responses to those effects.

HOW EXPLOSIVE ERUPTIONS AFFECT DRAINAGE BASINS

Emplacement of tephra and other volcanoclastic deposits occurs in three settings within drainage basins—on hillslopes, on valley floors (including active floodplains), and directly in streams and rivers (**Figure 1**). The impacts that the emplacement processes impose on these environments (e.g., Swanson & Major 2005) determine the degree of disturbance and the types and rates of geomorphic responses. The extent and degree of disturbance to a drainage basin generally scales with eruption magnitude, type of emplacement process, and proximity of the basin to the volcano. Proximal drainage basins within 10–20 km of erupting volcanoes commonly are affected enough to disrupt equilibrium conditions, but basins many tens or even hundreds of kilometers distant can be adversely affected if an eruption is large enough (e.g., Pareschi et al. 2000, Bell & House 2007, Manville et al. 2009b).

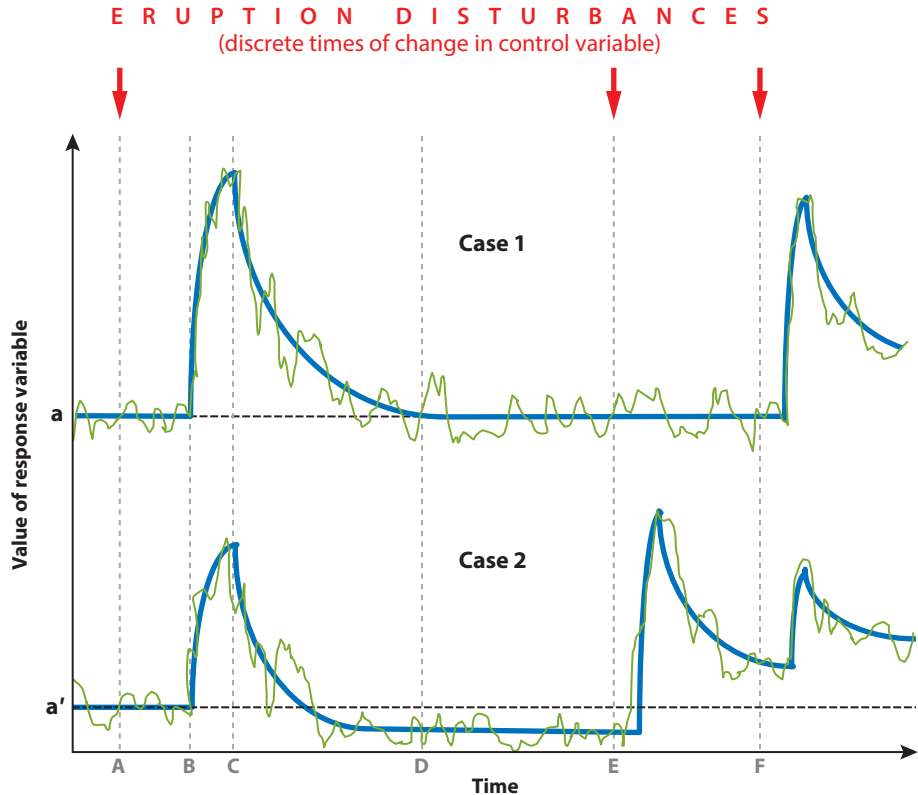


Figure 2

Schematic representation of change to a geomorphic variable (response variable) in a fluvial system, which is adjusting to a measure of disturbance (control variable) imposed by an explosive eruption (adapted from Graf 1977). The solid blue line represents the mean condition, and the solid green line represents short-term fluctuations. In a simple example represented by case 1, a variable in a disturbed system (such as channel-bed elevation) initially deviates from a pre-eruption steady-state value (value a) and then returns to a value similar to that in the pre-eruption condition. The drainage basin for case 1 is affected by volcanic disturbances at times A and F. Interval AB is the reaction time before the variable begins responding. Interval BC is the destabilization time, when the value of the response variable is moving away from the value characterizing pre-eruption stability. Interval CD is the relaxation time, when the variable moves back toward and asymptotically approaches the normative pre-eruption condition. Interval DF represents a period of steady-state equilibrium. In drainage basins where the imposed disturbances are volcanic eruptions, interval AD is also termed the syneruption period, and interval DF is termed the intereruption period (Smith 1991). In the more complex case 2 example, the drainage basin is affected by three eruptions at times A, E, and F. In this example, the response variable does not return to its original pre-eruption value (value a') or to later pre-eruption values, and at time F the eruption occurs before the variable has reached a steady-state value.

Tephra Fall

Falling tephra affects drainage basins principally in two ways: It kills, damages, or buries vegetation due to a variety of physical, chemical, and physiological effects, and it forms a nearly continuous landscape-mantling layer that is typically impermeable at the deposit surface yet easily erodible (Figure 3a). Both effects are critical for altering drainage-basin hydrology and sedimentation. Tephra fall can disturb much larger areas of terrain than can other volcanic processes (commonly $>10^3$ km² versus order 10^1 km²) (Manville et al. 2009b, Ayris & Delmelle 2012).

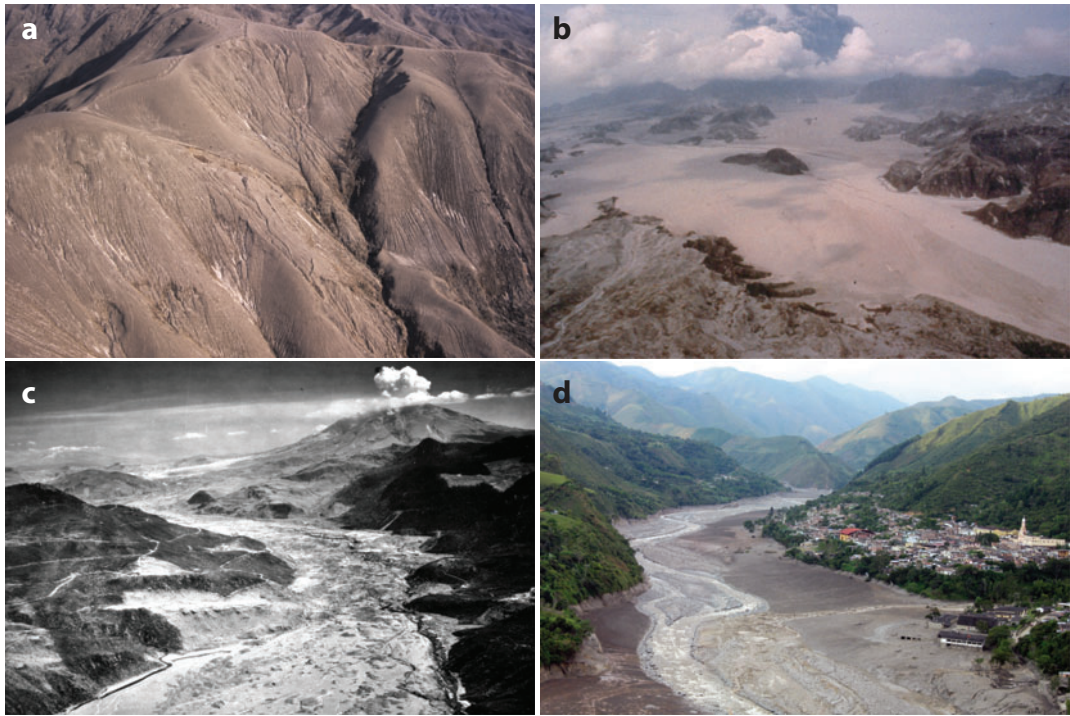


Figure 3

Views of landscape modifications caused by explosive volcanic eruptions. (a) Tephra-mantled hillslopes swept by pyroclastic density currents and mantled by tephra fall near Mount Pinatubo (Philippines), July 15, 1991. Note complete removal or burial of vegetation and beginning of rill erosion following initial rainfalls. Photograph by J.J. Major, US Geological Survey. (b) Valley-filling deposit of pyroclastic density currents up to 200 m thick at Mount Pinatubo, June 22, 1991. Photograph by R.P. Hoblitt, US Geological Survey. (c) Debris-avalanche deposit at Mount St. Helens (United States), June 30, 1980. Photograph by A. Post and R.M. Krimmel, US Geological Survey. (d) Channel modification at Belalcázar (Colombia) caused by lahar from eruption of Nevado del Huila volcano. Photograph by B.A. Pulgarín, Servicio Geológico Colombiano, November 30, 2008. All photographs are used with permission.

Tephra-fall deposits extend downwind from volcanoes, usually in elliptical patterns in which particle size and deposit thickness decline more or less exponentially with distance from the vent, but they can have more complicated patterns (Houghton et al. 2000, Bonadonna & Costa 2013). In the simplest eruptions, the coarsest and densest particles rain out first, followed by progressively finer particles. Short-lived, single eruptions commonly produce overall upward-fining tephra sequences, and the top layers can be composed of extremely fine ash (<0.063 mm; White & Houghton 2006). Deposits from a single eruption can vary from <1 mm to many meters thick. Tephra-fall deposits are unconsolidated, loose, and highly erodible, and because they are spread over large areas, large volumes of tephra can be eroded quickly during rainstorms.

Vegetation impacts imposed by tephra fall are determined by tephra particle size, deposit thickness, and chemical interactions. Coarse tephra can abrade and strip trees of foliage and branches, and accumulations of fine tephra in tree canopies can be heavy enough (particularly when wet) to break off large limbs and tree crowns (Waldron 1967, Chinen & Rivière 1990, Swanson et al. 2013). Damage to vegetation below the forest canopy depends in part on the height of understory plants and in part on the amount of tephra intercepted by the canopy, but tephra falls of even moderate thickness (5–10 cm) can significantly damage understory vegetation (Antos & Zobel 2005). Thin ash coatings on foliage have the potential to cause widespread leaf kill, which can result

in a prolonged rain of dead leaves onto tephra surfaces that can alter tephra-layer properties. Leaf kill may be due to (a) chemical damage from acid aerosol deposition (i.e., volcanic gas condensate carried as aerosol droplets adhering to ash particles) and release of water-soluble compounds from highly reactive particle surfaces, or (b) interference with leaf-surface metabolic activity, i.e., temperature regulation, gas and energy exchange, and photosynthesis (Cook et al. 1981, Mills 2000, Antos & Zobel 2005, Ayris & Delmelle 2012, Swanson et al. 2013). Thin ash coatings on leaves may be removed by rain or wind before causing damage, however (e.g., Swanson et al. 2013).

Pyroclastic Density Current

Pyroclastic density currents (PDCs) can devastate landscapes, ecosystems, and populations in their paths. Volumes can exceed 1,000 km³; deposits commonly extend 10–20 km from source but may advance as far as 200 km (Freundt et al. 2000). Direct effects of a PDC on a drainage basin are due to high temperature (100°C to nearly 700°C), high velocity (generally >10 m/s and not uncommonly >100 m/s), abrasion and impact by fast-moving rock particles, and burial of valley floors by hot deposits (Freundt et al. 2000, Wilson & Houghton 2000).

Like tephra falls, PDCs can cause widespread damage to vegetation and leave highly erodible deposits. Large PDCs can strip hillslopes of all vegetation and even some soil, fill trunk valleys with deposits up to a few hundred meters thick, dam tributary valleys, and rearrange drainage divides (e.g., Bacon 1983, Wilson 1985, W.E. Scott et al. 1996, Macias et al. 2004, Manville et al. 2009b, Hildreth & Fierstein 2012) (**Figure 3b**). Even small PDCs, confined to a single valley and extending only a few kilometers, can be very damaging. They can topple or break trees, strip away branches and foliage, and leave deposits tens of centimeters to several meters thick (Nakada et al. 1999, Kelfoun et al. 2000, Major et al. 2013).

PDC deposits are generally loose, highly erodible, and largely confined to valley floors. Exceptionally large and energetic PDCs, however, can mantle broad swaths of landscape. Where rivers are forced to erode through thick PDC valley fills, the deposits provide a long-term sediment supply (e.g., Daag & van Westen 1996, Manville et al. 2009b, Gran et al. 2011). However, thick, very hot deposits from voluminous PDCs can form internally welded (lithified) zones (Freundt et al. 2000), which can greatly decrease their erodibility.

Debris Avalanche

Debris avalanches typically thickly bury and devastate river valleys and alluvial plains close to volcanoes (McGuire 1996, Glicken 1996, Siebert 2002). Debris avalanches leave little sediment on the flanks of volcanoes; flow paths on steep slopes close to source may be stripped of all vegetation and some soil. Deposits confined to incised valleys can be up to ~200 m thick locally and can extend >20 km from source (**Figure 3c**). In undissected terrain, avalanche deposits are more typically fan shaped in planform, are thinner (tens of meters thick), and extend up to 10–15 km from source, although some have extended to much greater distances.

Debris-avalanche deposits are characteristically a mixture of two kinds of material (Glicken 1996): pervasively fractured but minimally deformed fragments of the source edifice (blocks that can be up to hundreds of meters in diameter and that commonly form small irregular hills or hummocks on the deposit surface); and highly crushed, mixed, and sheared rock fragments, mostly of sand- and gravel-sized particles. Large debris avalanches can emplace ≥ 1 km³ of sediment in river valleys (Siebert 2002), block tributary valleys (Voight et al. 1981, Siebert 2002), disrupt drainage patterns (Janda et al. 1984), and provide an enormous long-term sediment source (Major et al. 2000).

Lahar

Impacts from lahars are focused along river channels. Lahars commonly reach 10–30 km downstream from source volcanoes, and the largest can flow hundreds of kilometers before depositing or evolving into muddy water floods. On the steep flanks of volcanoes, lahars are highly damaging and can strip away vegetation along flow paths (including large trees). Lahar deposits, composed dominantly of unconsolidated sand and gravel, occur either as broad, thin (less than or equal to a few meters) sheets in undissected terrain or as narrow, meters-thick fills that pave channels (**Figure 3d**). Substantial deposition by large debris-flow lahars occurs primarily on slopes less than approximately 2–3° (Rodolfo 1989, Vallance & Scott 1997), but depositional zones are neither uniform nor precisely predictable (e.g., Procter et al. 2010). Deposits having very low silt and clay contents are readily erodible by streams, whereas those rich in fines, especially those with clay contents >5% by weight, can be compacted and somewhat resistant to erosion. Because deposits are typically only meters thick, they may provide only a moderate-term (years to a few decades) source of sediment to the rivers they affect (Major et al. 2000).

EFFECTS OF DISTURBANCE ON BASIN HYDROLOGY

The three most important effects of explosive eruptions on basin hydrology are ones that alter the production and routing of rainfall and snowmelt runoff: (*a*) damage to basin vegetation, which decreases (or eliminates) interception and evapotranspiration; (*b*) reduction of infiltration rates of meteoric water (rain, snowmelt) due to tephra deposition, which increases overland flow and decreases subsurface water storage; and (*c*) alteration of hydraulic properties of stream channels, which enables efficient transport of water and sediment. In combination, these three effects alter the magnitude and frequency of rainfall- and snowmelt-generated floods and change the rates of sediment transport in rivers. In addition, drainage networks can be disrupted, storage of water within basins can be altered (e.g., resulting in the formation or destruction of lakes), and the character of sediment-transporting flows can be highly altered. In basins proximal to volcanoes, all three of these effects influence hydrologic responses. At distal sites where tephra deposition is a few centimeters or less, however, reduced infiltration is likely to be the only effective hydrologic impact.

Impacts on Runoff Production and Flow Routing During Rainstorms

Rainstorms and snowmelt deliver water to drainage basins, where some of it evaporates, some goes into long-term groundwater storage, and some runs off into streams. After an eruption, the proportion of that water reaching streams (runoff) and the rate at which it reaches those streams depend not only on the characteristics of the rainstorm or the melting snowpack but also on the ability of vegetation and tephra layers to control the routes and rates of water movement on or in the ground.

Hydrologic effects of vegetation loss. Foliage and tree bark intercept and store water in proportion to their surface areas during rainstorms (and snowstorms), allowing it to evaporate (or sublimate) without ever reaching the ground. Loss of water-storage surface area, which is greatest in forests, alters the timing and routing of precipitation runoff to streams in two fundamental ways: More water falls directly and immediately onto the ground surface during storms, and in the case of rainfall, it falls with greater impact force; and evapotranspiration is reduced, thus potentially allowing soils to remain wetter, which affects subsurface storage and runoff pathways.

Numerous studies have shown that evaporation loss of rainfall by interception in forests is highly variable, depending on a host of factors related to forest type, structure, and tree density; factors

related to understory plant and litter layers; and climatic factors related to storm characteristics, wind, air temperature, and humidity (summarized in Crockford & Richardson 2000). Documented interception losses in healthy forests range from near 100% for low-intensity rainfall events (nearly all rainfall intercepted) to a few tens percent during high-intensity rainfalls. Interception losses can even have slightly negative percentages (more throughfall to the ground than total rain) owing to fog condensation and drip. Average interception losses measured in temperate conifer forests are approximately 10–40% of total rainfall. Values measured in tropical and subtropical rainforests are typically at the low end of this range, 10–25%, due to the preponderance of high-intensity, short-duration rainstorms in those climates. High-intensity storms in temperate conifer forests also have interception losses at the lower end of the average range, 15–20% (Reid & Lewis 2009). Thus, destruction of forest vegetation allows more (sometimes much more) precipitation to reach the ground surface during precipitation events.

Reduced infiltration capacity due to tephra deposition. Infiltration capacity, the limiting rate at which rainfall (or snowmelt) can soak into the ground, influences the partitioning of subsurface and surface (overland flow) runoff. Such partitioning of runoff is important, because surface runoff reaches streams faster than does subsurface runoff. Factors affecting infiltration include the permeability of the ground surface, surface slope and roughness, the volumetric rate of water reaching the ground surface, and subsurface water content (Tindall & Kunkel 1999). If rainfall intensity (or rate of snowmelt) exceeds infiltration capacity, infiltration-excess (or Hortonian) overland flow occurs. Both field and laboratory experiments have shown that tephra deposition can cause post-eruption infiltration capacities to be reduced by as much as 2 orders of magnitude compared with pre-eruption infiltration capacities, and direct runoff ratios (proportion of total precipitation moving downslope as surface runoff) can increase from near zero to as much as 0.9 (**Table 1**).

Particle size of tephra alone can radically alter the rate of water soaking into the ground. The finer the tephra, the greater the loss of infiltration capacity (**Figure 4**), and this effect occurs whether fine ash is encountered at the deposit surface or at depth (Miller & Gardner 1962). Particles of very fine to extremely fine ash (≤ 0.125 mm), even when mixed with coarser particles, can render a tephra layer much less permeable than the pre-eruption landscape surface (e.g., Swanson et al. 1983, Leavesley et al. 1989, Teramoto et al. 2006, Ogawa et al. 2007). Furthermore, fine ash layers need not be thick to have this effect—layers as thin as 2–5 mm can significantly affect infiltration. Two field experiments in Japan (Teramoto et al. 2006, Ogawa et al. 2007) showed that when such thin layers containing at least 20% (by weight) extremely fine ash (< 0.063 mm) were applied to bare ground that had a dominantly medium to coarse ash surface (only approximately 5% < 0.063 mm), surface runoff volumes doubled, even during relatively low-intensity rainstorms. In addition, runoff response time was more rapid—there was less delay between peak rainfall and peak runoff after treatment than before. Enhanced runoff owing to tephra deposition can be modulated, however, by layers of leaves within tephra-fall deposits, which can prevent tight packing and keep the tephra layer permeable (e.g., Kisa et al. 2013).

Physical and chemical processes that modify surfaces of tephra deposits also can decrease infiltration. Various mechanisms acting within a thin zone (1–5 mm) just below the surface of fresh tephra layers can form an infiltration-limiting crust or seal. These mechanisms include (a) particle disaggregation by raindrop impact and packing of pore spaces with translocated fine particles, (b) compaction and loss of porosity in tephra layers over time and with cycles of wetting and drying (potentially by as much as one-third of original thickness in fine tephra deposits), and (c) “washing in” of suspended silt- and clay-sized particles into surface pore spaces by surface runoff and temporary ponding of water on relatively flat-lying tephra deposits (Horton 1933, 1940; Segerstrom 1950; Cook et al. 1981; Römkens et al. 1990; Hendrayanto et al. 1995;

Table 1 Measured infiltration capacities and runoff ratios on hillslopes near volcanic vents at varying times following eruptions

Volcano	Deposit type	Pre-eruption infiltration capacity (mm/h)	Posteruption infiltration capacity (mm/h)	Median grain size of deposit, D ₅₀ (mm)	2-year return interval, 1-h rainfall intensity (mm)	10-year return interval, 1-h rainfall intensity (mm)	Time since eruption (years)	Direct runoff ratio	Data source
Mount Ūsu	Tephra fall	—	1.5	0.063–0.25	18	36	1	—	a, b
		—	10	—	—	—	3	—	b
		75–100	2–5	0.03	14	20	0.25	0.42–0.91	c, d, e
Mount St. Helens	Tephra fall	—	4–7	—	—	—	1	0.23–0.73	e
		—	2–10	—	—	—	0.4	—	f
		—	9–25	—	—	—	18	—	g
Mount Yakedake	Tephra fall	—	3	0.25	23	29	14	—	h
		—	~40–400	—	—	—	32	—	i
		—	—	—	—	—	16	0.21	j
Mount Unzen	Pyroclastic flow	—	—	—	—	—	34	0.068	j
		—	9–18	0.5–2	50	81	1.5–3	—	k, l
		—	18–45	0.5–2	50	81	4	—	k, l
Sakurajima	Tephra fall	110–150	12–35	0.063	—	—	—	—	l, m
		105	14	0.05	—	—	—	—	n
		—	—	—	—	—	2	0.16	j
Sakurajima	Tephra fall	100	15–53	0.08–0.3	44	—	Variable (quiet)	—	m
		100	9–24	0.08–0.3	44	—	Variable (active)	—	m

(Continued)

Table 1 (Continued)

Volcano	Deposit type	Pre-eruption infiltration capacity (mm/h)	Posteruption infiltration capacity (mm/h)	Median grain size of deposit, D ₅₀ (mm)	2-year return interval, 1-h rainfall intensity (mm)	10-year return interval, 1-h rainfall intensity (mm)	Time since eruption (years)	Direct runoff ratio	Data source
Parícutin	Preexisting soil	22	—	—	—	—	0–3	—	o
	Tephra fall	—	42	0.4	—	—	0–3	—	o
	Tephra fall	—	35	0.25	—	—	0–3	—	o
	Tephra fall	—	24	0.25	—	—	0–3	—	o
Miyakejima	Tephra fall	140–180	1	0.05	—	—	0	—	p, q
		—	—	—	—	—	3	0.1–0.6	q, r
Merapi	Tephra fall/pyroclastic flow	—	—	—	—	—	7–8	0.05–0.30	i
Irazú	Tephra fall	—	—	—	—	—	0	≥0.80	s

References: (a) Yamamoto et al. (1980); (b) Yamamoto & Imagawa (1983); (c) Johnson & Beschta (1980); (d) Hoblitt et al. (1981); (e) Leavesley et al. (1989); (f) Fiksdal (1981); (g) Major & Yamakoshi (2005); (h) Okuda et al. (1977); (i) Suwa & Sumaryono (1996); (j) Suwa & Yamakoshi (1999); (k) Yamakoshi & Suwa (2000); (l) Miyabuchi et al. (1999); (m) Shimokawa & Jirousono (1997); (n) Ikeya et al. (1995); (o) Segerstrom (1950); (p) Nomura et al. (2003); (q) Yamakoshi et al. (2005); (r) Tagata et al. (2006); (s) Waldron (1967). Dashes indicate that no data were provided by the cited source(s).

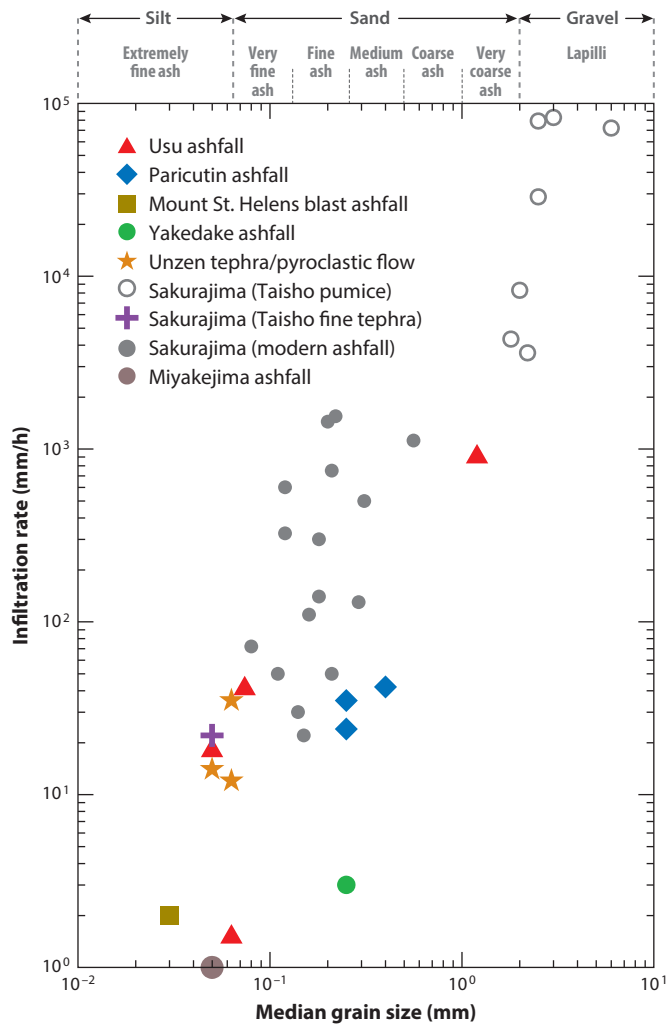


Figure 4

Relationships between infiltration rate and grain size of tephra-fall and pyroclastic-density-current deposits. Modified from Shimokawa et al. (1989).

Fohrer et al. 1999). In addition to these physical mechanisms, exchangeable sodium content of ash and underlying soil, electrolyte concentrations in rainfall, and chloride adhering to fresh ash particles can promote chemical dispersion of colloidal particles (if present) and formation of crusts on tephra-deposit surfaces by evaporative precipitation of soluble salts, which further inhibit infiltration (Waldron 1967, Cook et al. 1981, Römkens et al. 1990). Exchangeable sodium content of volcanic ash at Unzen volcano was noted to be higher than that in the local forest soils (Onda et al. 1996).

Antecedent water content of tephra, as well as the underlying soil, also influences infiltration rate. Infiltration rate decreases as interstitial water content increases (Horton 1940, Tindall & Kunkel 1999), owing to reduction of available pore volume, weaker hydraulic gradient with depth, and swelling of colloidal particles, if present. Thus, early wetting of a tephra layer (perhaps by a gentle rain following deposition) could further decrease infiltration capacity.

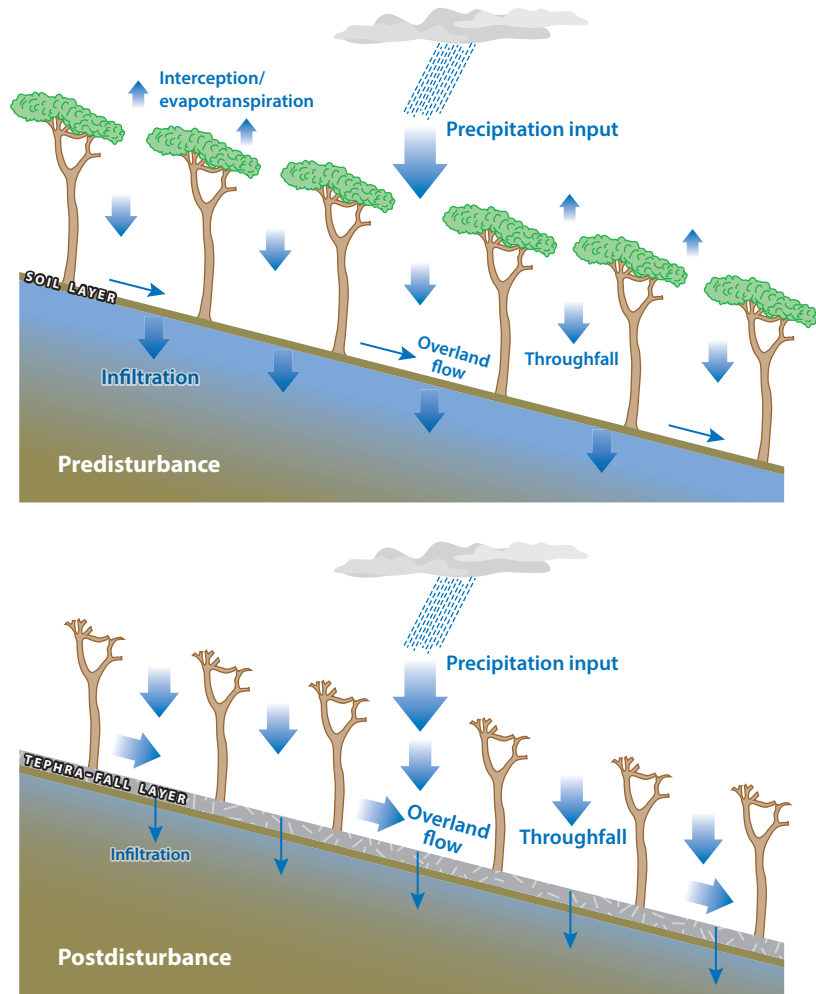


Figure 5

Conceptual diagrams of chief modes, pathways, and relative fluxes of water transfer during rainfall or snowmelt runoff, before and after volcanic disturbance. Width of arrows depicts relative magnitude of water transfer. In the posteruption diagram, note the loss of canopy interception, the greater amount of precipitation reaching the ground surface (throughfall), reduced evapotranspiration, reduced ground surface infiltration, and prominent overland flow.

In addition to altering surface infiltration, tephra fall also buries the pre-eruption litter layer and organic soil horizon on the forest floor. As a result, the hydraulically rough and permeable forest floor is replaced with a smooth and mostly impermeable ash pavement. The combination of more water reaching the ground surface because of vegetation damage and the nearly impervious pavement of tephra routing that water across the ground surface significantly increases the volume and rate of storm runoff from hillslopes (**Figure 5**).

Changes in channel character and continuity. When drainage networks are disrupted by valley-floor deposition by PDCs or debris avalanches, or rarely lahars, new channels must be developed on the featureless to chaotically rough surface topographies of the new valley fills

(Figure 3b,c). Unchanneled runoff may initially collect in random depressions that must fill with water and then overtop and drain before new channels can be carved. Furthermore, channel extension, commonly driven by knickpoint retreat, must occur for drainage networks to become fully integrated. Even after a new drainage network is able convey runoff, transported sediment may still get stored for a time in breached pond depressions, in temporary tributary impoundments, and along channels. Fully effective conveyance of water and sediment in a reestablished channel network across debris-avalanche and PDC deposits can take years to complete (Rosenfeld & Beach 1983, Daag & van Westen 1996, Simon 1999), and early postdisturbance channels are typically wider, steeper, and straighter than their buried predecessors (Meyer & Martinson 1989, Gran & Montgomery 2005). Lahar deposits, in contrast, typically do not rearrange drainage networks. Instead, they veneer existing topography. However, lahars commonly ream out riparian corridors, straighten channel alignments, and, because of their great sand loads, make channel beds hydraulically smoother (Figure 3d).

Impacts on Flood Discharges

Increased production rates and volumes of runoff resulting from reduced infiltration and interception of precipitation on basin hillslopes, together with hydraulically smoother channels on valley floors, lead to larger flood peaks and faster flood-peak rise times (Orwig & Mathison 1982, Datta et al. 1983, Branch 1991, Todesco & Todini 2004, Favalli et al. 2006, Major & Mark 2006, Yamakoshi et al. 2006). Numerous field studies report anomalously large flash floods and lahars immediately following eruptions (e.g., Waldron 1967, Janda et al. 1984, Suwa & Yamakoshi 1999, Lavigne 2004, Yamakoshi et al. 2005, Manville et al. 2009b, Alexander et al. 2010), and even low-intensity rainstorms cause unusually large (and highly sediment-laden) floods and lahars when proportions of runoff are high relative to total rainfall (Kadomura et al. 1983, Yamakoshi et al. 2005, Tagata et al. 2006, Alexander et al. 2010, Pierson et al. 2013).

Stream discharge responses to rainstorms vary with disturbance characteristics. Following the May 18, 1980, eruption of Mount St. Helens, modeling studies showed that peak discharges of unit hydrographs would be 50–200% greater and have rise times 25–30% faster than those of pre-eruption unit hydrographs (Orwig & Mathison 1982, Branch 1991). [A unit hydrograph is the hydrograph of storm runoff having a volume of one unit (millimeter, centimeter, or inch) of equivalent depth distributed over a basin, generated by a relatively short-duration rainstorm of uniform intensity.] They also predicted that magnitudes of floods of given frequencies would be 20–60% larger than under pre-eruption conditions, with changes greatest for small- to moderate-magnitude events (Lettenmaier & Burges 1981, Branch 1991). Major & Mark (2006) showed, however, that posteruption flow peaks were more complex and varied with respect to season, event magnitude, nature of volcanic disturbance, and time since eruption. The disturbance effects on flow peaks were strongest from basins in which both hillslope hydrology and channel hydraulics were altered by eruption processes, and weakest from basins in which only hillslope hydrology was affected, and then only transiently, by thin to moderate tephra-fall deposits. Amplification of event peaks was most pronounced in autumn following onset of the rainy season. Autumn flow peaks across a range of magnitudes (from event peaks less than mean annual flow to those greater than the 10-year return-interval flood) were amplified by several to many tens percent above pre-eruption flow peaks for a period of approximately 5 years, and amplified to a lesser extent for up to a decade in the most heavily disturbed basin. In general, in basins in which both hillslope hydrology and channel hydraulics were altered, both small- and large-magnitude peaks were amplified nearly proportionately, whereas in basins in which only hillslope hydrology was altered, small- to moderate-magnitude peaks were amplified more relative to large peaks.

Such dependency of flow-peak response on type of basin disturbance, season, and flow magnitude shows that hydrological responses to disturbance can be complex. It further suggests that changes to channel hydraulics, and not just hillslope runoff, can play a prominent role in the hydrological response (Major & Mark 2006).

EFFECTS OF DISTURBANCE ON BASIN SEDIMENTATION

Delivery of large volumes of unconsolidated volcanoclastic sediment to drainage basins, together with subsequent erosion and secondary transport of that sediment, leads to sediment transport dominated by lahars and high-concentration floods, to increased sediment yields, and to major geomorphic changes to stream channels in those basins (Smith 1991). The type and degree of sedimentation response depend on the initial sediment emplacement process; the volume, character, and distribution of volcanoclastic debris; the local climate; and the physiography and hydrology of the affected landscape and its ability to store sediment. Magnitude and duration of sedimentation responses increase as the degree of landscape disturbance increases.

Erosion Mechanisms and Sediment Sources

Sediment delivered to rivers in drainage basins disturbed by explosive eruptions comes from two basic sources (**Figure 6**): from hillslopes, where it is mobilized by sheet and rill erosion and by shallow landsliding of widely dispersed tephra-fall and PDC deposits; and from more localized valley-fill PDC, debris-avalanche, and lahar deposits, where it is mobilized by sheet and rill erosion from fill surfaces and by incision and lateral erosion of reestablishing stream channels. (The term rill is used broadly here to connote a relatively shallow, typically steep-sided channel eroded by the concentrated flow of surface runoff during rainstorms or rapid snowmelt. Such channels deeper or wider than approximately 1 m are also commonly termed gullies.) Sediment delivery from these sources occurs at different rates and persists for different durations (Major et al. 2000, Gran et al. 2011). Not only are freshly emplaced deposits eroded by these processes, but significant quantities of older hillslope and valley-fill deposits are commonly mobilized as well (e.g., Waldron 1967; Pierson et al. 1990, 1996; Swanson & Major 2005).

Erosion from hillslopes. Sheet and rill erosion are dominant processes on hillslopes, because most or all of the early posteruption precipitation and snowmelt runs off as overland flow (Segerstrom 1950; Waldron 1967; Kadomura et al. 1983; Swanson et al. 1983; Chinen 1986; Collins & Dunne 1986; Takeshita 1987; Shimokawa et al. 1989, 1996; Leavesley et al. 1989; Yamakoshi et al. 2002; Waythomas et al. 2010; Pierson et al. 2013). Rill networks typically are initiated by the first significant rains following tephra emplacement, and erosion rate commonly accelerates initially for a year or two as the cumulative length, depth, and density of rills increase (Schneider et al. 2013). Rills flush sediment quickly and efficiently to valley floors and streams, because hillside rills are steep and more or less straight (**Figure 6e**) and because flow in rills typically has high sediment concentrations, sometimes occurring as miniature debris flows (Segerstrom 1950).

Sediment production from rills on hillslopes is rapid but limited. Volcanic ash is easily erodible in most cases, and rills can incise fairly quickly (sometimes within days to months) down to erosion-resistant substrates, such as a buried soil or lava flow, or to coarser, more permeable tephra layers. When such substrates are encountered, tephra erosion decreases dramatically (e.g., Collins & Dunne 1986). Furthermore, once rills stop incising, the rill network evolves toward fewer but larger master rills and more connectivity between rills (e.g., Swanson et al. 1983, Schneider et al. 2013). As rills evolve, biogenic and cryogenic processes commonly loosen tephra-deposit surfaces

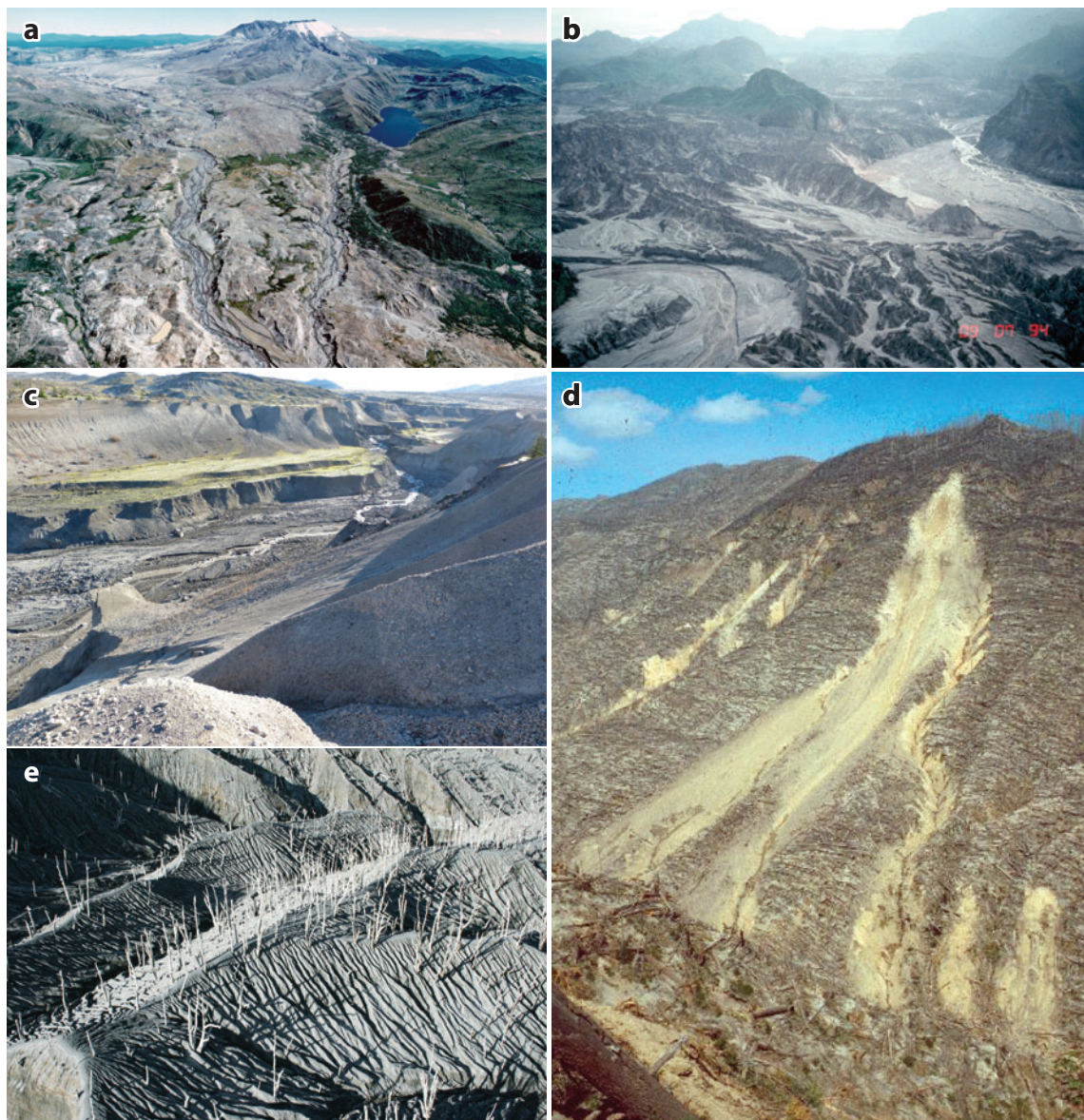


Figure 6

Examples of erosion of volcanic deposits. (a) Erosion of Mount St. Helens (United States) debris-avalanche deposit and consequent channel development; a debris-dammed lake (Castle Lake) is visible at the upper right. Compare with **Figure 3c** (same location). Photograph courtesy of Washington State Department of Transportation; taken prior to 1992. (b) Erosion of thick pyroclastic-density-current fill at Mount Pinatubo (Philippines). Compare with **Figure 3b** (same location). Photograph by C.G. Newhall, US Geological Survey, September 7, 1994. (c) North Fork Toutle River channel cut into 1980 debris-avalanche deposit at Mount St. Helens. Note steep banks that can easily be undercut by high flows. Photograph by K.R. Spicer, US Geological Survey, November 21, 2013. (d) Shallow landslides in blast pyroclastic-density-current deposit at Mount St. Helens. Photograph by Fred Swanson, US Forest Service, summer 1982. (e) Rill erosion in tephra-mantled hillslope near Chaitén volcano (Chile), January 21, 2010. Photograph by T.C. Pierson, US Geological Survey. All photographs are used with permission.

in tandem with rill incision, allowing sheetwash and wind deflation to more effectively remove fines and increase mean grain size (e.g., Swanson et al. 1983, Yamamoto 1984). Coarsening of deposit surfaces in conjunction with biogenic and cryogenic dilation of sediment at depth allows infiltration capacities to increase, with less flow partitioned to surface runoff. Surface coarsening, rill stabilization, and network evolution can swiftly reduce high posteruption sediment yields from hillslopes by 1–2 orders of magnitude (Chinen 1986, Collins & Dunne 1986, Major et al. 2000, Yamakoshi & Suwa 2000). A rapid decline in sediment production from tephra-mantled hillslopes generally occurs within a few years of an eruption and can occur even in the absence of revegetation (Chinen 1986, Collins & Dunne 1986), although sediment-production rates can stay above background rates for many years. For example, erosion rates (primarily from rills) were approximately 50% above typical background rates at Parícutin volcano (México) 50 years after the 1943 eruption (Inbar et al. 1994), and higher-than-normal sediment releases from disturbed basins in Iceland have persisted for decades (Hardardóttir et al. 2001). In some cases, frequent eruptions persistently recharge slopes (and channels) with tephra, and extremely large volumes of sediment can continue to be released for long periods (Shimokawa et al. 1989, Harris et al. 2006).

Rapid stabilization of rill networks means that large volumes of tephra can remain in place on hillslopes following eruptions, although climatic factors and other variables may affect the fraction remaining. For example, in drainage basins at Usu volcano and Mount St. Helens, only approximately 10–20% of the tephra volumes deposited from eruptions in 1977–1978 and 1980, respectively, were removed within 1–4 years of tephra emplacement before rill networks became stabilized and erosional processes reverted to those more typical of temperate forested landscapes (e.g., soil creep and mass wasting) (Kadomura et al. 1983, Chinen 1986, Collins & Dunne 1986, Smith & Swanson 1987). At Irazú—a tropical volcano receiving intense rainfall—an estimated 30–50% of newly deposited tephra was eroded by the end of the 1964 rainy season during the 1963–1965 eruption (Waldron 1967). Tephra from older eruptions remaining on hillslopes may, however, be eroded and mobilized following subsequent volcanic disturbances.

In addition to rill erosion, landsliding (both shallow and deep-seated) is also an effective process for eroding fresh and older tephra on hillslopes (Seegerstrom 1950, 1960; Waldron 1967; Kadomura et al. 1983; Swanson et al. 1983; Smith & Swanson 1987; Takeshita 1987; Pareschi et al. 2000) (**Figure 6d**). It occurs where hillslopes are steep, where tephra layers are sufficiently fine grained to become saturated during intense or prolonged rainstorms (e.g., Swanson et al. 1983, Pierson et al. 1996), and where hillslopes or terraces are undercut by accelerated erosion in stream channels (Waldron 1967). The efficacy of landslides as a sediment source depends on a number of factors, including the recurrence intervals and durations of sufficiently intense rainstorms, thicknesses and layering of tephra accumulations, and, on forested hillslopes, a competition between the timescales of root decomposition of trees killed by an eruption and recolonization of new forest. A time window of enhanced vulnerability to landsliding starts once roots of trees killed by an eruption begin to decay and lose the strength necessary to anchor older soil and tephra on slopes; minimum strength typically occurs roughly 7–10 years after tree death in coniferous stands (Ziemer 1981). The window ends when the new roots of recolonizing trees become sufficiently strong to restabilize the slope (e.g., Johnson & Wilcock 1998, Swanson & Major 2005). Loss of soil shear strength due to tree-root decay can be critical for slopes mantled by progressively weathering (and weakening) tephra layers. At Mount St. Helens, for example, widespread shallow landsliding of 1980 and older tephra delivered large volumes of sediment to stream valleys during a heavy rainstorm 16 years after the eruption (Swanson & Major 2005).

Erosion from valley floors. Erosion of valley-filling or landscape-burying PDC or debris-avalanche deposits produces greater and more prolonged sedimentation responses than does

erosion of hillslope tephra or relatively thin lahar deposits. This greater and longer response occurs because streams incise and widen new or existing channels; adjust channel geometries to posteruption, higher-discharge flow regimes; and maintain persistent lateral adjustments commonly for decades, not just for a few years (Major et al. 2000, Kataoka et al. 2009, Manville et al. 2009b, Gran et al. 2011, Gran 2012). Posteruption channel adjustments vary with the type of new deposit emplaced on the valley floor, but in general they follow complex cycles of incision, aggradation, and widening (Meyer & Martinson 1989, Daag & van Westen 1996, Simon 1999).

Initial posteruption channel erosion in thick valley-fill deposits can be rapid and dramatic (**Figure 6a–c**). This is especially true where volcanoclastic deposits have overwhelmed and reconfigured drainage-basin topography. Full-scale sediment mobilization, however, requires that drainage networks first be reestablished and reintegrated. In some instances, drainage reintegration can lead to piracy and dramatic changes in basin area, which can have significant downstream repercussions (e.g., K.M. Scott et al. 1996, Pringle & Scott 2001, Daag & van Westen 1996, Manville et al. 2009b). For example, channels developed on the Mount St. Helens debris-avalanche deposit and on the thick pyroclastic fill at Mount Pinatubo incised tens of meters and widened hundreds of meters within the first year following the respective eruptions (Meyer & Martinson 1989, Daag & van Westen 1996). At El Chichón (México), valleys buried in PDC deposits by an eruption in 1982 were incised up to 20 m within 8 years, but most of that incision occurred within the first few months after the eruption (Inbar et al. 2001). But even in smaller-volume valley-fill deposits emplaced by lahars, immediate posteruption channel instability can be severe. Lahar-affected channels at Mount St. Helens, and at Merapi and Semeru (Indonesia), which were filled with only a few meters of lahar deposits, responded initially by incising up to several meters, widening by tens of meters, and then locally aggrading by several meters (Meyer & Martinson 1989, Lavigne 2004).

Prolonged channel erosion that follows the initially rapid adjustments to emplacement of large-volume valley fills is mainly the result of relatively minor but persistent mining of bed and bank sediment by the river (Gran & Montgomery 2005, Gran et al. 2011). Initial channel incision commonly exposes high, steep banks and terrace sides to undercutting and mass failure. High flows along such channels easily entrain the typically sandy sediment masses that have toppled or slumped into the active channel. Such channels are also typically very mobile. They can easily migrate laterally and induce further bank erosion, remobilization of bed sediment, and sometimes renewed incision (Gran 2012). In some cases, prolonged lateral erosion can release valley-fill sediment that has been in storage for centuries.

Effects on Sediment Transport

Large sediment inputs to drainage basins by eruptions clearly increase the volume of material available to transport but also increase the rate of sediment transport in rivers. The added sediment causes channel conditions and sediment-transporting processes to evolve to promote greater transport efficiency and higher sediment fluxes. Concentrations of sediment-transporting flows increase, and channel beds become smoother, steeper, and straighter. These effects increase sediment-transport capacity over a wide range of discharges.

A major effect of landscape disturbance by explosive eruptions is that lahars become more frequent. Occurrence of tens to hundreds of lahars can dominate posteruption sediment transport in many volcanic settings for several years, particularly in tropical climates (Waldron 1967, Imagawa 1986, Hirao & Yoshida 1989, Rodolfo 1989, Umbal 1997, Suwa & Yamakoshi 1999, Lavigne 2004, Lavigne & Suwa 2004, Gran & Montgomery 2005, Yamakoshi et al. 2005, Harris et al. 2006, Manville et al. 2009b). In other cases, more typically in nontropical climates, only

one or two lahars may occur and fluvial processes then dominate early posteruption sediment delivery (e.g., Major 2004; Pierson et al. 2011, 2013). Lahars are important because they can carry 10 to 20 times more sediment than can the muddiest postdisturbance water floods, as shown in sediment-concentration data from Mount St. Helens and Mount Pinatubo (Fairchild 1987, Hayes et al. 2002, Major 2004, Pierson 2005), and suspended-sediment concentrations in postdisturbance streamflows from disturbed basins can be up to 100 times higher than they are in streamflows from undisturbed basins (Davies et al. 1978, Janda et al. 1984, Montgomery et al. 1999, Hayes et al. 2002, Major 2004, Favalli et al. 2006).

When lahars are not occurring, most posteruption sediment delivery and redistribution occur during seasonal high flows (e.g., Major 2004). In severely disturbed basins, however, small storm flows and even seasonal low flows can redistribute exceptional amounts of sediment owing to the high sediment concentrations (Montgomery et al. 1999, Hayes et al. 2002, Pierson et al. 2013). Not only do higher-concentration streamflows carry more sediment (both suspended load and bed load), but their higher fluid densities make them more erosive, more hydraulically efficient, and more capable of entraining additional sediment (e.g., Coleman 1986, Pierson 2005, Cloutier et al. 2006).

Hydraulic smoothing of channels results from the massive deposition of sand that is triggered by large sediment inputs. Deposited sand can bury armor-layer gravel on channel beds, thereby decreasing channel roughness. Such fining and smoothing of the channel bed enhance flow efficiency and increase sediment transport (Montgomery et al. 1999, Gran et al. 2006, Gran 2012). Transport increases because effective basal shear stresses exerted by streamflow are greater on a smooth channel bed, and critical shear stresses needed to mobilize sediment are smaller, compared with rougher gravel beds (e.g., Wilcock & Crowe 2003). As a result, excess shear stress (the difference between effective and critical shear stress) is large, and bed material can be more easily entrained and transported (Montgomery et al. 1999, Gran et al. 2006). Extraordinary transport rates of sandy bed load in volcanically disturbed systems help maintain reduced channel roughness until the supply of sand declines (Gran et al. 2006).

The channel gradient of a river increases when large inputs of sediment raise bed elevation in the upper part of the basin. Recent experiments have shown that bed slope and mean shear stress increase directly with increasing sediment supply, which increases transport rate by a factor of approximately 2.5 (Podolak & Wilcock 2013). In a field example, the massive debris-avalanche deposit from the 1980 eruption of Mount St. Helens increased the average gradient of the upper North Fork Toutle River, the source of extraordinarily elevated sediment-transport rates (Major et al. 2000), by 0.006 m/m over a 25-km-long reach (Simon 1999). Straightening of channel alignments, especially by lahars, not only contributes to increased channel gradient by shortening the channel but also reduces flow resistance derived from channel sinuosity. Increases in channel gradient and decreases in planform resistance add to the effect of hydraulic smoothing of the channel bed to increase flow velocity, which can nudge a river from lower-regime (turbulent subcritical) flow to critical or upper-regime (turbulent supercritical) flow and thereby greatly increase sediment-transport capacity. This flow-regime transition is important, because critical to upper-regime flow imposes higher basal shear stresses on channel beds than does lower-regime flow (Grant 1997).

Sediment Routing Within Drainage Basins

Volcaniclastic sediment, once it is eroded and entrained, moves downslope and downstream at varying volumetric rates, by different flow processes (mass-flow or fluvial) and by direct or indirect paths. The amount of sediment produced within or delivered to a drainage basin (sediment input) must balance the amount that is discharged from the basin (sediment output), plus the positive or

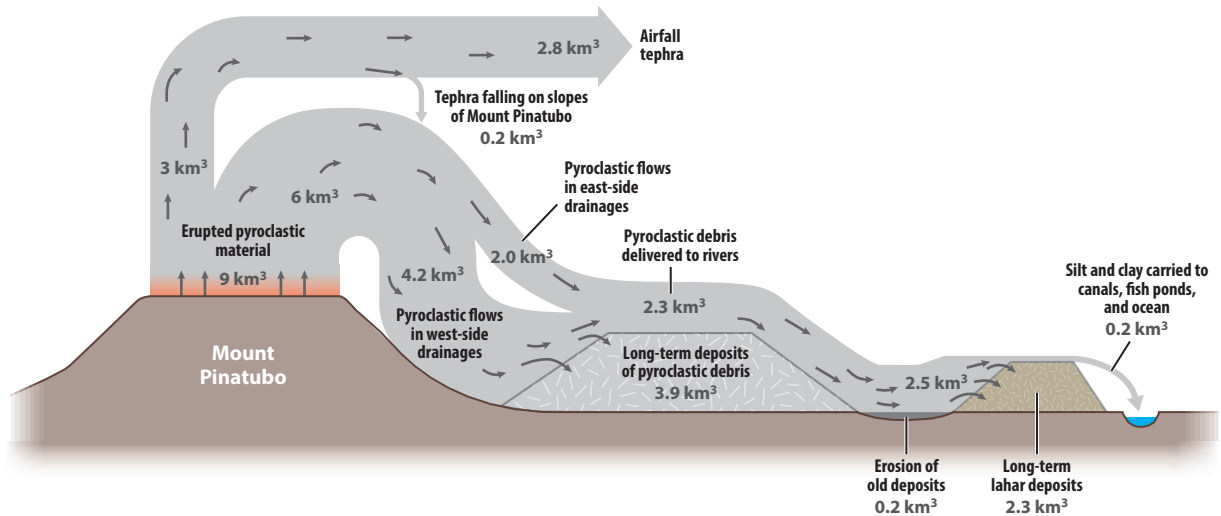


Figure 7

Example of a sediment-routing flow diagram for drainage basins on and near Mount Pinatubo (Philippines). Most of the sediment went into storage in these basins in the first year following the 1991 eruption. After the eruption, lahars were initially the dominant sediment-transporting process. From Pierson et al. (1992).

negative change in volume of sediment stored within the basin (sediment storage), or $I = O + \Delta S$ (Swanson et al. 1982). Sediment storage can occur in a variety of locations: on hillslopes, on fans at the bases of slopes, in mass-movement deposits, in alluvial fills or terraces, and in the beds of active channels. How the downstream sediment flux varies with time and how sediment is partitioned to storage, both encompassed in the term sediment routing, depend on basin characteristics and processes as well as on the character and quantity of both input sediment and older sediment already in storage (Dietrich et al. 1982). Volcaniclastic sediment routing within a basin can be depicted conceptually and semiquantitatively as a flow diagram (Figure 7). The rate at which sediment leaves a drainage basin (usually expressed as $\text{Mg km}^{-2} \text{ year}^{-1}$ or $\text{m}^3 \text{ km}^{-2} \text{ year}^{-1}$) is termed sediment yield, which can also be viewed as a long-term, basin-wide, average erosion rate.

The relative proportions of ΔS and O can be quite different in basins receiving large inputs of volcaniclastic sediment. Davies et al. (1978) reported that in the year 1976, following small explosive eruptions of Fuego volcano (Guatemala) in 1971, 1973, and 1975 and a major explosive eruption in October 1974, 27% of the sediment input to the adjacent Achiguate River basin ($1,322 \text{ km}^2$) went into storage and 73% reached the sea as sediment output. In contrast, during the first year following the 1991 eruption of Mount Pinatubo, an estimated 97% of all of the sediment input to basins heading on the volcano went into storage and only approximately 3% reached higher-order basins or the sea (Pierson et al. 1992). This disparity in sediment storage is probably a function of the magnitude of sediment input, but it is also a function of distance and average gradient between the source volcanoes and the basin mouths; channels are longer and flatter at Pinatubo (50–120 km and 0.012–0.029 m/m) than at Fuego (60 km and 0.063 m/m).

The concept of excess sediment. When volcanic eruptions, and subsequent erosion processes, deliver extraordinary volumes of sediment to a drainage basin network, stream channels must adjust. As discussed above, adjustments include changes in channel gradient, fining and smoothing of the bed, increased sediment-transport efficiency, and, if a river system is loaded with more sediment than it can carry (i.e., its transport capacity is exceeded), increased sediment storage

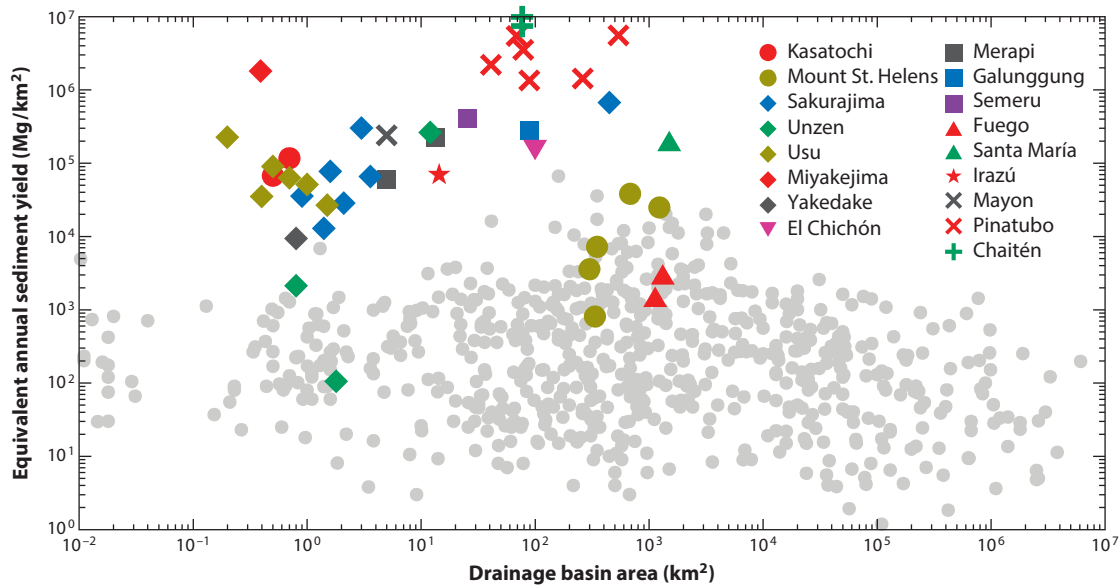


Figure 8

Average annual (mostly suspended) sediment yield as a function of drainage basin area for yields from volcanically disturbed basins and nonvolcanic river basins worldwide. Data sources for plotted sediment yields are provided in **Supplemental Table 1** and accompanying references; follow the **Supplemental Materials link** in the online version of this article or at <http://www.annualreviews.org>.

Colored data points are for drainage basins affected by recent volcanic eruptions. Gray data points are for basins in volcanic terrain where no recent eruptions have occurred and in nonvolcanic terrain.

Supplemental Material

along the channel and valley floor. Adjustments also include changes in channel form. The amount of sediment exceeding that which kept a river in its former equilibrium condition can be thought of as excess sediment. Some excess sediment increases yield from the basin, and some goes into storage within the basin.

Erosion rates and sediment yields. Erosion of fresh volcanoclastic material, augmented by erosion of sediment that has been stored for perhaps centuries in a basin, can generate unit-area sediment releases that rival those of the greatest sediment-transporting rivers worldwide (see **Figure 8** and **Supplemental Table 1**; follow the **Supplemental Materials link** in the online version of this article or at <http://www.annualreviews.org>). Even though extraordinary posteruption sediment transport is transitory within the broader geological history of a basin, it can dominate decadal-scale to centennial-scale (and rarely millennial-scale) sediment budgets in volcanic drainage basins (Umbal 1997, Major et al. 2000, Manville & Wilson 2004, Gran et al. 2011). Disturbed volcanic basins can debouche sediment at rates in excess of 10^6 m³/day (Kuenzi et al. 1979, Pierson et al. 2013), and when converted to average rates of landscape denudation, erosion rates of volcanically disturbed basins typically exceed those of other basins by 3–4 orders of magnitude (**Supplemental Table 1**).

Sediment yields vary with the nature of volcanic disturbance, even from the same eruption (**Figure 9**). Sediment delivery from zones of channel disturbance is greater and persists longer than that from zones of hillslope disturbance. Although sediment yields from volcanically disturbed basins initially can be several hundred times greater than typical pre-eruption yields (Major et al. 2000, Gran et al. 2011), they commonly diminish rapidly within a few years of disturbance (e.g.,

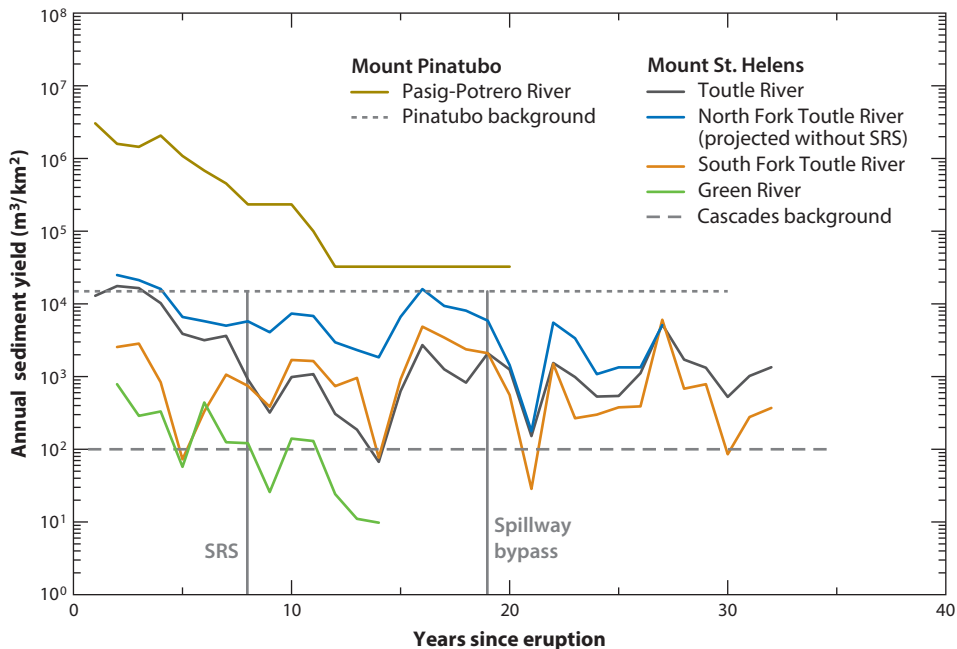


Figure 9

Comparison of sediment yields from severely disturbed basins at Mount St. Helens (United States) and Mount Pinatubo (Philippines) as functions of time since eruption. The point in time labeled SRS represents the time that the US Army Corps of Engineers completed a large sediment retention structure on the North Fork Toutle River, Washington, which trapped both bed load and suspended load. Approximately 10 years after SRS completion, sediment began passing over the structure spillway. Data for North Fork Toutle River are adjusted to account for sediment trapped by SRS. Mount St. Helens sediment yields are based on suspended-sediment data only, whereas Mount Pinatubo data come mainly from measurements of accumulated deposits and thus represent both suspended-load and bed-load sediment. Note the rapid decline of sediment yield within the first 5 to 10 years after each eruption. Modified from Major et al. (2000) and Gran et al. (2011).

Simon 1999, Suwa & Yamakoshi 1999, Major et al. 2000, Lavigne 2004, Yamakoshi et al. 2005, Gran et al. 2011). Declines in yield follow exponential curves initially for approximately the first 5–10 years (**Figure 9**) (Chinen 1986, Pierson et al. 1992, Major et al. 2000, Lavigne 2004, Gran et al. 2011), which is typical for disturbed fluvial systems (Graf 1977, Schumm & Rea 1995). But before returning to background yield values, sediment yields from severely disturbed basins can persist at elevated levels for decades (e.g., **Figure 2**, case 2), owing to erosion from ongoing channel adjustments. At Mounts St. Helens and Pinatubo, posteruption yields from severely disturbed basins initially declined exponentially but then leveled off at fluctuating rates averaging an order of magnitude greater than estimated pre-eruption yields, and those elevated rates have been maintained more than 30 and 20 years, respectively, after those eruptions (**Figures 8 and 9**).

These two phases of elevated sediment yield—acute high magnitude and chronic lower magnitude—from heavily impacted drainage basins have been modeled conceptually (Gran et al. 2011) as two stages in fluvial-system response (**Figure 10**). During the first stage, initially extraordinary yields are attributed to rapid erosion of tephra from hillslopes and erosion of valley networks. Once supplies of easily erodible sediment are depleted, system response enters a second stage in which lower-level but persistent sediment release results from continued channel

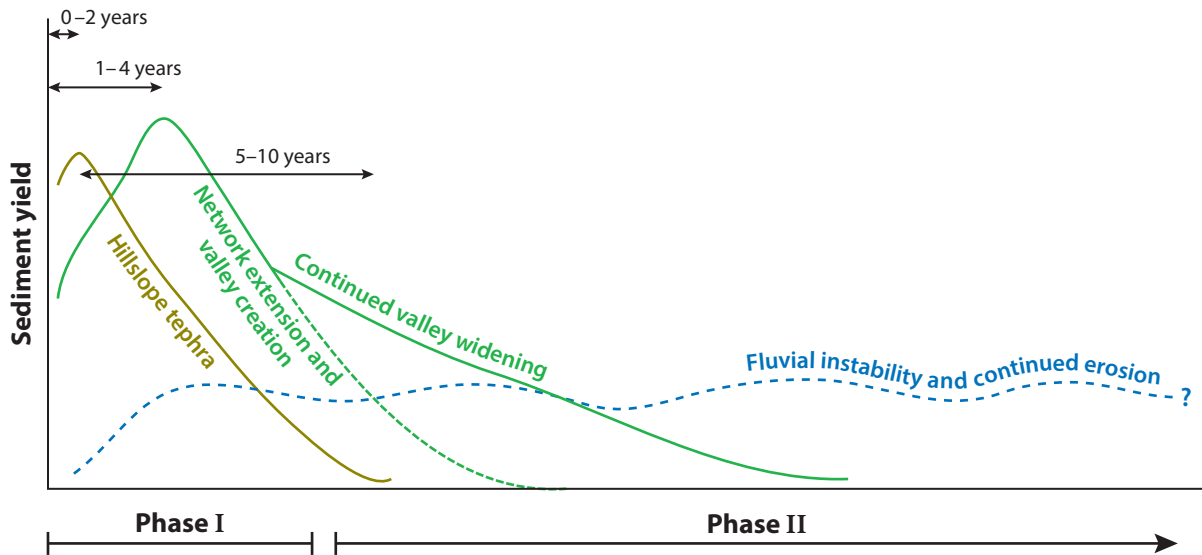


Figure 10

Conceptual diagram illustrating phases of geomorphic change and sources for sediment yield from volcanically disturbed basins, as functions of time and degree of basin recovery. Phase I response is caused by erosion of tephra from hillslopes and development of channel networks. This phase releases the greatest peak yields, but they decline rapidly. Phase II response is caused by persistent lower-level erosion related chiefly to ongoing channel widening and continued fluvial instability, which can continue for decades. Modified with permission from Gran et al. (2011).

instability owing to bed and bank erosion and from mass wasting from terraces developed during channel-network incision. However, as reestablished channels continue to widen, channel banks and terraces become less important sediment sources because the river has less contact with them. At that time, sediment mining from the channel bed becomes a principal source of sediment, but only as long as streamflows have the power to incise and access the sediment in bed storage.

Remobilization of channel-bed sediment is a function of both overall sediment supply and sand supply. Gran & Montgomery (2005) showed that bed armoring and channel stability at Mount Pinatubo occurred when input of sand-sized sediment to channels diminished. Armoring and channel stability first began to develop during seasonal low flows, then continued over the full range of seasonal flows. Development of clast structures on channel beds increased roughness and critical shear stress, reducing sediment transport. Further analysis by Gran et al. (2006) showed that a diminished input of sand to Pinatubo's river systems was the critical factor driving changes in bed texture, and Gran (2012) showed that seasonal sand loading produced seasonal responses in bed textures and sediment transport. Persistent sand loading during the rainy season disrupted and removed the armor layer that had developed during the dry season, and this led to the replacement of single-thread channels with braided channels. In turn, braided-channel development drove lateral river migration and channel bank erosion, which contributed additional sand to the system. This feedback mechanism thus kept the channel in a highly mobile state during the rainy season. Seasonal sand loading at Pinatubo, a process likely to occur at other volcanoes, led to complex cycles of incision and lateral migration that helped maintain persistently high sediment yields, even though excess shear stresses available to transport sediment had declined over time. Gran (2012) has proposed that deeper channel incision, and hence persistent mining of the channel bed, may be promoted by periodically disrupting and removing the armor layer.

GEOMORPHIC RESPONSES TO ALTERED HYDROLOGY AND EXCESS SEDIMENT

Increased flood magnitude and frequency, coupled with increased sediment-transport rates and sediment supply, trigger geomorphic responses in fluvial systems. Net accumulation of sediment in streams causes channels to fill in with bed-material sediment (mostly sand and gravel), which raises bed elevation; this process is termed channel aggradation (**Figure 11**). Aggradation in turn triggers changes in planform channel pattern, channel form (cross-sectional dimensions), and channel position within the floodplain. Waning of excess sediment supply readjusts the balance between water flow and sediment transport, allowing streams to lower bed elevation by downcutting, primarily through previously accumulated sediment; this process is termed channel degradation.

Channel Aggradation and Degradation

Channel aggradation generally occurs relatively quickly (over hours to years) in response to sediment loading, whereas degradation is more protracted (typically over years to decades). Timescales of aggradation and degradation depend on the volume, characteristics, and placement of the new sediment within the basin, on eruption frequency, and on basin morphology (**Supplemental Tables 2 and 3**). An aggradation phase combined with a degradation phase is termed an aggradation-degradation cycle (Smith 1991, Nicholas et al. 1995, Lisle et al. 2001). However, raising and lowering of the channel bed is not synchronous along the entire longitudinal profile. The mass of excess sediment may be translated downstream as a bulk-material wave, or it may be dispersed as a downstream-thinning sediment wedge. Bulk downstream movement of sediment depends on interactions between channel morphology, flow, and sediment-size and sediment-transport characteristics (Lisle et al. 2001).

Posteruption maximum aggradation levels vary widely and appear to be controlled as much by basin and channel morphology as by sediment input volume. Documented peak aggradation levels have ranged from a few meters to nearly 40 m in river reaches up to 100 km from source for sediment input volumes of 0.1 to 4 km³ (**Supplemental Table 3**). Posteruption aggradation of 5–10 m is extremely common, and except where truly massive sediment inputs were involved, aggradation levels >20 m are limited to bedrock-confined valleys 0.1–0.6 km wide. Both lahars and normal fluvial processes contribute to channel aggradation in reaches <50 km from sediment source (**Supplemental Table 3**), whereas beyond approximately 50 km aggradation is caused mainly by fluvial processes. This difference emphasizes the importance of lahars as a postdisturbance sedimentation process in proximal river reaches. Lag times from disturbance onset to attainment of peak aggradation level downstream can vary from days to years when a combination of lahar and fluvial deposition is involved (**Supplemental Table 3**).

Changes in Channel Pattern, Form, and Position

A river channel invariably responds to channel aggradation by changing from a single-thread channel pattern (straight, meandering, or anabranching) to a braided pattern (e.g., Davies et al. 1978, Kuenzi et al. 1979, Smith 1987, Gran 2012) (**Figure 11f**). Braiding, characterized by the formation of midchannel bars and multiple flow threads, occurs in response to aggradation and channel steepening that result from increased sediment supply (Schumm 1985). Channel pattern can also be affected by localized accumulations of large woody debris (log jams), which can be a direct result of forest destruction and downstream transport of logs by PDCs, lahars, or debris avalanches (e.g., Lisle 1995, Major et al. 2013, Swanson et al. 2013). Woody debris can deflect flow and influence sediment storage (Lisle 1995, Wohl 2013).

 [Supplemental Material](#)



Development of braided-channel patterns leads to major increases in active-channel and active-floodplain widths and decreases in channel depths. Such channel widening can be accompanied by rapid bank erosion. On low-gradient alluvial aprons and plains, syneruption braided-channel width/depth ratios commonly range from 100 to 400 (Davies et al. 1978, Kuenzi et al. 1979), and channels may be up to 300–400 m wide (Davies et al. 1978, Kesel & Lowe 1987). In contrast, steeper channels on volcano flanks and at fan heads are typically incised and relatively narrow: They are <25 m wide and have width/depth ratios in the 10–40 range (Davies et al. 1978, Kuenzi et al. 1979, Kesel & Lowe 1987). Width/depth ratios of comparable rivers in undisturbed basins in temperate climatic settings commonly range from approximately 10 to 100 (Dunne & Leopold 1979, Rosgen 1994).

Steep-gradient entrenched channels give way to lower-gradient unconfined or moderately confined braided channels anywhere from 20 to 60 km downstream of volcanoes depending on the physiographic setting (Kuenzi et al. 1979, Kesel & Lowe 1987, Newhall & Punongbayan 1996, Pierson et al. 2011). In-channel deposition and braiding generally commence at channel gradients of <0.01–0.03 m/m (Kesel & Lowe 1987, Rodolfo et al. 1996, Pierson et al. 2011).

Avulsion (whole or partial diversion of flow from an existing channel to a new channel or channels) is common in channels carrying high sediment loads. It appears to be triggered when aggradation is locally faster than lateral erosion and the bed is raised more than one channel depth above the surrounding floodplain (Jerolmack & Mohrig 2007). Avulsion can result in the shifting of a channel from one side of a floodplain to the other or from an existing channel through the middle of a town (e.g., Pierson et al. 2013) within hours.

RECOVERY OF DRAINAGE BASINS FOLLOWING DISTURBANCE

Drainage-basin recovery can be defined from various perspectives (e.g., hydrology, geomorphology, forest ecology, stream invertebrate ecology, pedology) (Major et al. 2000, Swanson & Major 2005, Dale et al. 2005, Gran & Montgomery 2005, Major & Mark 2006, Pierson et al. 2011). From a hydrogeomorphic perspective, we define it as the postdisturbance achievement by a basin's fluvial system of a state of balance among average water flux, average sediment flux, and adjustable measures of channel morphology and sediment transport (response variables) (**Figure 2**). Recovery does not require return to a system's pre-eruption condition; rather, it requires the achievement of a steady-state condition, whether new or old, in balance with posteruption boundary conditions and mass and energy inputs. The period of disequilibrium (syneruption period) following most eruptions lasts for years to decades (e.g., Kesel & Lowe 1987, Major et al. 2000, Gran et al. 2011).

Figure 11

Examples of downstream sedimentation caused by erosion of volcanic sediment from disturbed basins. (*a,b*) Aggradation (after 3 months) on the Boyong River at Merapi volcano (Indonesia). The bridge in panel *a* stands 7 m above the channel bed. From Lavigne et al. (2000). (*c,d*) Sedimentation along the Bambang River at Mount Pinatubo (Philippines). Nearly 9 m of sediment deposition occurred during a single lahar event. From Punongbayan et al. (1996). (*e*) Fluvial sedimentation at Chaitén town following eruption of Chaitén volcano (Chile). Note how the river has avulsed through town and built a large delta into Chaitén Bay. Photograph by E. Manríquez, December 2010. (*f*) Braided channel of the Rayas River in a drainage basin heavily affected by tephra deposition during the explosive phase of the 2008–2009 eruption of Chaitén volcano. The volcano is visible in the upper-right corner of the photograph, with a steam cloud hanging over the growing lava dome. Photograph by T.C. Pierson, US Geological Survey, January 2010. (*g*) Thick fluvial fill along the lower Sandy River, Oregon, related to the reworking of lahar and pyroclastic-density-current deposits from an eruption of Mount Hood (United States) in the late 1700s. The section exposes trees that were rapidly buried in growth position. The level of the surface on which the trees were growing is just above the man's knees. Photograph by T.C. Pierson. All photographs are used with permission.

Following very large eruptions or frequent, ongoing eruptions, syneruption periods may last for centuries or, rarely, millennia (Manville & Wilson 2004, Manville et al. 2009b). Disturbance effects (particularly from large eruptions) can be complex, and geomorphic responses can be delayed (White et al. 1997, Kataoka et al. 2009).

In general, the more severely a fluvial system has been disturbed, the longer it takes to reestablish an equilibrium condition. Some volcanically disturbed systems may never fully achieve a steady-state condition but only tend toward one after each disturbance, either because eruptions are too frequent (e.g., Sakurajima volcano) or additional overlapping nonvolcanic disturbances may be imposed (e.g., sediment pulses resulting from accelerated erosion due to tree kill from insect infestation, wildfires, logging, land-use changes, or short-term climate cycles). Furthermore, multiple potential equilibrium states may exist for a fluvial system (Phillips 2009, Wu et al. 2012).

Hydrologic Recovery

Hydrologic effects of vegetation destruction and loss of infiltration capacity on basin hillslopes can remain for decades (Major & Yamakoshi 2005), but the most extreme effects typically last for only a few years (Kadomura et al. 1983, Chinen 1986, Collins & Dunne 1986, Suwa & Yamakoshi 1999, Yamakoshi & Suwa 2000, Yamakoshi et al. 2005). For example, infiltration capacities that had been reduced by as much as 2 orders of magnitude following eruptions of Mount St. Helens and Unzen volcanoes were increased again 2- to 5-fold within 1 to 3 years after eruptive disturbance (Leavesley et al. 1989, Jitousono et al. 1996). Similarly, suspended-sediment yield from a basin disturbed by the blast PDC of the 1980 Mount St. Helens eruption had declined significantly within 5 years, which was attributed mainly to increased infiltration capacity and reduced surface runoff (Major et al. 2000).

After about a decade, most disturbed drainage basins begin to function hydrologically more or less as they did prior to disturbance, as direct runoff ratios decrease to 0.3 or less (e.g., Leavesley et al. 1989, Suwa & Sumaryono 1996, Suwa & Yamakoshi 1999, Tagata et al. 2006; see also **Table 1**). Regrowth of vegetation aids in hydrologic recovery and can be extremely rapid where moisture is abundant, particularly if roots and other plant tissues buried by tephra remain viable and new shoots are able to sprout through a relatively thin tephra deposit (Swanson et al. 2013). In arid climates, in contrast, volcanoclastic deposits can remain essentially barren for decades or even centuries (e.g., in the Andean altiplano). Nonetheless, complete hydrologic recovery of hillslopes can be slow. Major & Yamakoshi (2005) found that whereas plot-specific infiltration capacities on an eruption-disturbed hillslope at Mount St. Helens (revegetated mainly by grasses and shrubs) had increased 5- to 10-fold after 20 years, the measured rates still remained 3 to 5 times slower than predisturbance rates. Thus, despite major movement in the direction of recovery, this site had not yet fully recovered hydrologically to pre-eruption conditions, and some winter-storm rainfall intensities could still exceed surface infiltration capacity and cause surface runoff (**Table 1**).

The formation of lakes through tributary blockage by mass-flow deposits can extend the hydrologic legacy of eruptive disturbances years to decades beyond the time window of hydrologic recovery on hillslopes (White et al. 1997, Manville et al. 2007). Failures of lake-impounding natural dams produce lahars or floods that can renew downstream channel instability and rejuvenate erosion in headwater areas and tributary channels. In contrast, debris-dammed lakes may survive to be part of an evolving new steady-state condition (e.g., Kuenzi et al. 1979, Scott 1988, Willingham 2005).

Geomorphic Recovery

Geomorphic recovery generally involves the stabilization of channel pattern and form, establishment of an armored channel bed, and development of a characteristic hydraulic geometry. A

geomorphically stable fluvial system also is reflected by a characteristic range in sediment yield. Following volcanic eruptions, achievement of geomorphic stability can be complicated by large-scale stream piracy, by lake breakouts, and by shifting climatic patterns (Daag & van Westen 1996, Umbal 1997, White et al. 1997, Major et al. 2000, Manville et al. 2009b) (**Figures 9 and 10**). Recent studies have tracked the trajectory of geomorphic recovery following disturbance of volcanic fluvial systems:

1. **Mount Pinatubo, Philippines, and Mount St. Helens, United States: Initial exponential decline of sediment yield followed by a plateau at elevated levels.** The most recent summary of postdisturbance recovery in the Pasig-Potrero/Sacobia River drainage basin following the 1991 eruption of Mount Pinatubo (Gran et al. 2011) (**Figure 9**) shows a decade-long exponential decline in sediment yield after the eruption, followed by 8 years of yields elevated 2 to 10 times above estimated predisturbance yields. A 32-year record for rivers at Mount St. Helens similarly shows nearly a decade of exponential sediment-yield decline (**Figure 9**), followed by a plateau of fluctuating yield values, sensitive to annual variations in winter-storm characteristics and averaging up to an order of magnitude above predisturbance yield values. These fluvial systems appear to still be in a disequilibrium condition.
2. **Mount St. Helens, United States: Inconsistent indicators of fluvial system stability.** The >20-year-long plateau of elevated sediment yields at Mount St. Helens noted above was accompanied by continued bank erosion and channel avulsion; both are commonly considered to be indicators of instability. That apparent instability occurred simultaneously with an exponential decline in the rate of change of bed elevation (Zheng et al. 2014), which has been noted as an indicator of achievement of a new equilibrium condition. Thus, volcanic fluvial systems can exhibit inconsistent signs of geomorphic stability and instability even decades after disturbance.
3. **Mount Hood, United States: Possible lingering effects of previous disturbances.** The most recent period of volcanically related heavy sediment loading of the upper Sandy River basin occurred in the late eighteenth century and resulted in a brief (<12-year) period of channel aggradation (≥ 23 m) along a river reach 70 km downstream of the volcano (Pierson et al. 2011). This was followed by a longer relaxation period (50–100 years) of channel incision and the achievement of a new and apparently stable bed elevation (confirmed in 1911), a well-armored streambed, and a dominantly single-thread channel pattern. However, a 2011 winter rainstorm triggered a flood that caused vigorous localized aggradation, lateral erosion, and channel avulsion in the upper Sandy River, which indicated greater channel instability in this river than in similarly sized rivers in adjacent drainage basins during the same storm. One important difference between the upper Sandy and upper reaches in adjacent basins is that large volumes of volcanoclastic sediment, a legacy of eruptive periods approximately 200 and 1,500 years ago, form channel-bounding high terraces in the upper Sandy River. Those terraces are mined episodically by high flows and provide sufficient sediment loading to trigger channel instability. Thus, it may be that only a condition of metastability was achieved in the late nineteenth century, rather than a more robust steady-state condition.
4. **Santa María volcano, Guatemala: Complications of continued volcanic activity.** Following this volcano's large explosive eruption in 1902, Río Samalá sediment yield increased, and within a year caused channel widening, development of a braided-channel pattern, channel aggradation and lateral shifting, formation of debris-dammed lakes, and progradation of a river delta (Kuenzi et al. 1979). For more than a century, this fluvial system has remained highly unstable with sediment yields approximately 5 times above pre-eruption values owing to persistent shedding of sediment by the still-active Santiaguito lava dome, which started growing at this volcano in 1922 (Kuenzi et al. 1979, Harris et al. 2006).

Definitive documentation of full geomorphic recovery of volcanically disturbed basins remains elusive, at least for recent eruptions. However, documented recovery trajectories in basins heavily loaded by sediment from mining activity (James 1991) and geologic studies of recovery from older eruptions (Manville & Wilson 2004, Manville et al. 2009b) suggest that full geomorphic recovery can take at least several decades following minor disturbances and centuries to millennia following major disturbances.

ADDITIONAL VOLCANO-HYDROLOGIC HAZARDS

Explosive eruptions and associated processes are hazardous in their own right, but fluvial systems responding and adjusting to such volcanic disturbances can impose additional hazards on downstream communities up to 100 km or more from a volcano (Kataoka et al. 2009, Manville et al. 2009b). Increased vulnerability of communities downstream of volcanoes arises principally from two potential direct and indirect effects of sediment-producing volcanic disturbances: (a) blockage of tributary streams or lake outlets by newly emplaced deposits and the consequent impoundment of lakes (or raising of existing lake levels) by unstable natural dams (**Figures 1b** and **6a**), and (b) infilling of river channels with excess sediment as channels aggrade (**Figures 1b** and **11**). Both these effects can lead to increased flooding and potentially large secondary lahars. As impounded lakes fill, upstream communities can be submerged by backflooding, and if the blockage is catastrophically breached, lake-breakout floods (which commonly transform into lahars) may threaten communities far downstream (Scott 1988, Umbal & Rodolfo 1996, White et al. 1997, Macías et al. 2004, Manville et al. 2007). Floods or lahars from such lake breakouts can occur years to decades after the blockage was formed (White et al. 1997, Manville et al. 2007, Procter et al. 2010). Channel aggradation can partly or entirely fill an active channel with sand and gravel, reducing or eliminating channel capacity and increasing the magnitude and frequency of flooding (Lombard et al. 1981). Aggradation also allows a river to migrate across its floodplain or even an entire valley floor, where roads, homes, vehicles, agricultural land, and forests can be flooded and buried in sediment.

SUMMARY

Large explosive volcanic eruptions cause widespread and damaging disturbances to surrounding landscapes. They affect drainage basins primarily by destroying vegetation and depositing large volumes of fine-grained volcaniclastic particles over broad areas. The principal eruption-related processes that disturb landscapes include tephra fall, pyroclastic density currents, and eruption-triggered lahars. Other processes associated with explosive eruptions and also capable of delivering large volumes of volcaniclastic sediment to drainage basins include dome-collapse block-and-ash flows, edifice-collapse debris avalanches, syneruption rain-triggered lahars, and lake-breakout lahars. The degree and severity of disturbance to a drainage basin are functions of the specific volcanic disturbance process, as well as proximity to the volcano and magnitude of the eruption.

Drainage basins affected by explosive eruptions typically exhibit much higher rates and volumes of precipitation runoff than do similar unaffected basins. These hydrologic effects result from (a) large-scale destruction of vegetation, particularly forest vegetation, which decreases precipitation interception and evapotranspiration, and (b) the widespread deposition of fine volcanic ash, which reduces hillslope infiltration rates by several orders of magnitude and increases the proportion of surface runoff. As a result of these effects, meteorologic floods tend to occur more frequently and have higher peak discharges than they did prior to disturbance.

Affected drainage basins also respond to disturbance with rates of sediment erosion and transport much higher than those of similar unaffected basins. Syneruption unit-area sediment yields

are among the highest in the world. One reason is that highly erodible tephra is widely distributed over basin hillslopes and along channels and is primed for rapid erosion by the increased surface runoff. Another reason is that lahars play an important role in eroding, entraining, and transporting sediment in disturbed basins both during eruptions and for several years thereafter. Such high-concentration flows are comparatively rare in undisturbed drainage basins.

Eruption-induced changes to basin hydrology and sedimentation disrupt the preexisting geomorphic stability in drainage basins and induce changes to river profiles, channel patterns and dimensions, and sediment-transport processes. Recovery of a disturbed fluvial system to a reestablished stable (or metastable) geomorphic condition typically takes decades to centuries, depending on the nature and degree of basin disturbance and on the criteria used to define stability.

The volcanic and volcano-hydrologic processes that emplace volcanoclastic sediment in drainage basins can create new hazards for downstream communities as basins adjust to large sediment inputs. Blockage of tributary streams or lake outlets by newly emplaced deposits and the consequent impoundment of lakes (or raising of existing lake levels) can lead to backflooding upstream of blockages and to large lake-breakout floods and lahars downstream. Infilling of river channels with excess sediment increases the frequency and magnitude of flooding, and it can redirect fluvial erosion and deposition to vulnerable areas. These hazards can affect broad areas extending to 100 km or more downstream of volcanoes.

There have been significant recent advances in our understanding of how drainage basins are affected by and respond to explosive eruptions, particularly since the 1980 eruption of Mount St. Helens. However, more work is needed to convert these advances into predictive models that can assist emergency managers with decisions regarding which communities downstream of active volcanoes to evacuate (and when) and assist planners in zoning vulnerable river valleys for future development.

DISCLOSURE STATEMENT

The authors are not aware of any affiliations, memberships, funding, or financial holdings that might be perceived as affecting the objectivity of this review.

ACKNOWLEDGMENTS

Our review of this topic is based on a large number of studies worldwide and supplemented by our own field work, site visits, and discussions and collaborations with many colleagues over the courses of our careers. Many more papers beyond those we are able to cite have contributed to our understanding of the subject. Their omission reflects space limitation, not our lack of appreciation of their contributions; their citations may be found in the bibliographies of many of the broader-perspective papers that we do cite. We are thankful for the constructive criticism received from Tom Dunne, James White, and others for this review, and especially for help from Japanese colleagues Takao Yamakoshi and Hiroshi Suwa for assistance in tracking down data and references in Japanese-language sources.

LITERATURE CITED

Alexander J, Barclay J, Sušnik J, Loughlin SC, Herd RA, et al. 2010. Sediment-charged flash floods on Montserrat—the influence of synchronous tephra fall and varying extent of vegetation damage. *J. Volcanol. Geotherm. Res.* 194:127–38

- Anderson T, Flett JS. 1903. Report on the eruptions of Soufrière, in St. Vincent, in 1902, and on a visit to Montagne Pelée in Martinique—Part 1. *Philos. Trans. R. Soc. A* 200:353–553
- Antos JA, Zobel DB. 2005. Plant responses in forests of the tephra-fall zone. See Dale et al. 2005, pp. 47–58
- Ayris PM, Delmelle P. 2012. The immediate environmental effects of tephra emission. *Bull. Volcanol.* 74:1905–36
- Bacon CR. 1983. Eruptive history of Mount Mazama and Crater Lake caldera, Cascade Range, USA. *J. Volcanol. Geotherm. Res.* 18:57–115
- Bell JW, House PK. 2007. Did Plinian eruptions in California lead to debris flows in Nevada? An intriguing stratigraphic connection. *Geology* 35:219–22
- Belousov A, Behncke B, Belousova M. 2011. Generation of pyroclastic flows by explosive interaction of lava flows with ice/water-saturated substrate. *J. Volcanol. Geotherm. Res.* 202:60–72
- Belousov A, Voight B, Belousova M. 2007. Directed blasts and blast-generated pyroclastic density currents: a comparison of the Bezymianny 1956, Mount St. Helens 1980, and Soufrière Hills, Montserrat 1997 eruptions and deposits. *Bull. Volcanol.* 69:701–40
- Bonadonna C, Costa A. 2013. Modeling tephra sedimentation from volcanic plumes. In *Modeling Volcanic Processes: The Physics and Mathematics of Volcanism*, ed. SA Fagents, TKP Gregg, RMC Lopes, pp. 173–202. Cambridge, UK: Cambridge Univ. Press
- Branch WE. 1991. Hydrologic change caused by the eruption of Mount St. Helens. In *Irrigation and Drainage, Proceedings of the 1991 National Conference*, ed. WF Ritter, pp. 531–38. New York: Am. Soc. Civ. Eng.
- Branney MJ, Kokelaar P. 2002. *Pyroclastic Density Currents and the Sedimentation of Ignimbrites*. Geol. Soc. Lond. Mem. 27. London: Geol. Soc. Lond. 143 pp.
- Cashman KV, Sparks RSJ. 2013. How volcanoes work: a 25 year perspective. *GSA Bull.* 125:664–90
- Chinen T. 1986. Surface erosion associated with tephra deposition on Mt. Usu and other volcanoes. *Environ. Sci. Hokkaido* 9(1):137–49
- Chinen T, Rivière A. 1990. Post-eruption erosion processes and plant recovery in the summit atrio of Mt. Usu, Japan. *Catena* 17:305–14
- Cloutier D, LeCouturier MN, Amos CL, Hill PR. 2006. The effects of suspended sediment concentration on turbulence in an annular flume. *Aquat. Ecol.* 40:555–65
- Coleman N. 1986. Effects of suspended sediment on open-channel velocity distribution. *Water Resour. Res.* 22(10):1377–84
- Collins BD, Dunne T. 1986. Erosion of tephra from the 1980 eruption of Mount St. Helens. *GSA Bull.* 97:896–905
- Cook RJ, Barron JC, Papendick RI, Williams GJ III. 1981. Impact on agriculture of the Mount St. Helens eruptions. *Science* 211:16–22
- Crockford RH, Richardson DP. 2000. Partitioning of rainfall into throughfall, stemflow and interception: effect of forest type, ground cover and climate. *Hydrol. Process.* 14:2903–20
- Czuba JA, Magirl CS, Czuba CR, Grossman EE, Curran CA, et al. 2011. *Sediment load from major rivers into Puget Sound and its adjacent waters*. USGS Fact Sheet 2011-3083, US Dep. Inter., USGS, Wash. Water Sci. Cent., Tacoma, WA
- Daag A, van Westen CJ. 1996. Cartographic modeling of erosion in pyroclastic flow deposits of Mount Pinatubo, Philippines. *ITC J.* 2:110–24
- Dale VH, Swanson FJ, Crisafulli CM, eds. 2005. *Ecological Responses to the 1980 Eruption of Mount St. Helens*. New York: Springer. 342 pp.
- Datta B, Lettenmaier DP, Burges SJ. 1983. *Assessment of changes in storm and seasonal runoff response of watersheds impacted by Mt. St. Helens ash deposition*. Water Resour. Ser. Tech. Rep. 82, Dep. Civ. Eng., Univ. Wash., Seattle
- Davies DK, Vessell RK, Miles RC, Foley MG, Bonis SB. 1978. Fluvial transport and downstream sediment modifications in an active volcanic region. In *Fluvial Sedimentation*, ed. AD Miall, pp. 61–84. Can. Soc. Pet. Geol. Mem. 5. Calgary, Can.: CSPG
- Dietrich WE, Dunne T, Humphrey NF, Reid LM. 1982. Construction of sediment budgets for drainage basins. See Swanson et al. 1982, pp. 5–23
- Dunne T, Leopold LB. 1979. *Water in Environmental Planning*. New York: Freeman. 818 pp.

- Fairchild LH. 1987. The importance of lahar initiation processes. In *Debris Flows/Avalanches: Process, Recognition, and Mitigation*, ed. JE Costa, GF Wicczorek, pp. 51–62. GSA Rev. Eng. Geol. 7. Boulder, CO: GSA
- Favalli M, Pareschi MT, Zanchetta G. 2006. Simulation of syn-eruptive floods in the circumvesuvian plain (southern Italy). *Bull. Volcanol.* 68:349–62
- Fiksdal AJ. 1981. Infiltration rates of undisturbed and disturbed Mount St. Helens tephra deposits. *Wash. Geol. Newsl.* 9(3):1–3
- Fohrer N, Berkenhagen J, Hecker J-M, Rudolph A. 1999. Changing soil and surface conditions during rainfall—single rainstorm/subsequent rainstorms. *Catena* 37:355–75
- Folk RL. 1980. *Petrology of Sedimentary Rocks*. Austin, TX: Hemphill. 184 pp.
- Freundt A, Wilson CJN, Carey SN. 2000. Ignimbrites and block-and-ash flow deposits. See Sigurdsson et al. 2000, pp. 581–99
- Glicken HX. 1996. *Rockslide-debris avalanche of May 18, 1980, Mount St. Helens Volcano, Washington*. USGS Open-File Rep. 96-677, US Dep. Inter., USGS, Cascades Volcano Obs., Vancouver, WA. 90 pp.
- Graf W. 1977. The rate law in fluvial geomorphology. *Am. J. Sci.* 277:178–91
- Gran KB. 2012. Strong seasonality in sand loading and resulting feedbacks on sediment transport, bed texture, and channel planform at Mount Pinatubo, Philippines. *Earth Surf. Process. Landf.* 37:1012–22
- Gran KB, Montgomery DR. 2005. Spatial and temporal patterns in fluvial recovery following volcanic eruptions—channel response to basin-wide sediment loading at Mount Pinatubo, Philippines. *GSA Bull.* 117:195–211
- Gran KB, Montgomery DR, Halbur JC. 2011. Long-term elevated post-eruption sedimentation at Mount Pinatubo, Philippines. *Geology* 39:367–70
- Gran KB, Montgomery DR, Sutherland DG. 2006. Channel bed evolution and sediment transport under declining sand inputs. *Water Resour. Res.* 42:W10407
- Grant GE. 1997. Critical flow constrains flow hydraulics in mobile-bed streams: a new hypothesis. *Water Resour. Res.* 33:349–58
- Hardardóttir J, Geirsdóttir A, Thordarson T. 2001. Tephra layers in a sediment core from Lake Hestvatn, southern Iceland: implications for evaluating sedimentation processes and environmental impacts on a lacustrine system caused by tephra fall deposits in the surrounding watershed. In *Volcaniclastic Sedimentation in Lacustrine Settings*, ed. JDL White, NR Riggs, pp. 225–46. Spec. Publ. Int. Assoc. Sedimentol. 30. Oxford: Blackwell Sci.
- Harris AJL, Vallance JW, Kimberly P, Rose WI, Matías O, et al. 2006. Downstream aggradation owing to lava dome extrusion and rainfall runoff at Volcán Santiaguito, Guatemala. In *Volcanic Hazards in Central America*, ed. WI Rose, GJS Bluth, MJ Carr, JW Ewert, LC Patino, JW Vallance, pp. 85–104. GSA Spec. Pap. 412. Boulder, CO: GSA
- Hayes SK, Montgomery DR, Newhall CG. 2002. Fluvial sediment transport and deposition following the 1991 eruption of Mount Pinatubo. *Geomorphology* 45:211–24
- Hendrayanto, Kobashi S, Mizuyama T, Kosugi K. 1995. Hydrological characteristics of new volcanic ash deposit. *J. Jpn. Soc. Hydrol. Water Resour.* 8(5):484–91
- Hildreth W, Fierstein J. 2012. *The Novarupta-Katmai Eruption of 1912—Largest Eruption of the Twentieth Century: Centennial Perspectives*. USGS Prof. Pap. 1791. Washington, DC: USGS. 259 pp.
- Hirao K, Yoshida M. 1989. Sediment yield of Mt. Galunggung after eruption in 1982. *Proc. Int. Symp. Eros. Volcan. Debris Flow Technol., July 31–Aug. 3, Yogyakarta, Indonesia*, V21-1–V21-22. Yogyakarta, Indones.: Minist. Public Works
- Hoblitt RP, Miller CD, Vallance JW. 1981. Origin and stratigraphy of the deposit produced by the May 18 directed blast. See Lipman & Mullineaux 1981, pp. 401–20
- Horton RE. 1933. The role of infiltration in the hydrologic cycle. *Trans. Am. Geophys. Union* 14:446–60
- Horton RE. 1940. An approach toward a physical interpretation of infiltration-capacity. *Proc. Soil Sci. Soc. Am.* 5:399–417
- Houghton BF, Wilson CJN, Pyle DM. 2000. Pyroclastic fall deposits. See Sigurdsson et al. 2000, pp. 555–70
- Ikeya H, Hendrayanto, Kosugi K, Mizuyama T. 1995. Observed changes in the infiltration rates of pyroclastic deposits resulting from volcanic activities. *J. Jpn. Soc. Eros. Control Eng.* 48(2):22–26 (in Japanese, with English abstr.)

- Imagawa T. 1986. Mud and debris flows on Mt. Usu after the 1977–1978 eruption. *Environ. Sci. Hokkaido* 9(1):113–35
- Inbar M, Enriquez AR, Graniel JHG. 2001. Morphological changes and erosion processes following the 1982 eruption of El Chichón volcano, Chiapas, Mexico. *Geomorphol. Relief Process. Environ.* 3:175–84
- Inbar M, Hubp JL, Ruiz LV. 1994. The geomorphological evolution of the Parícutin cone and lava flows, Mexico, 1943–1990. *Geomorphology* 9:57–76
- James LA. 1991. Time and the persistence of alluvium: river engineering, fluvial geomorphology, and mining sediment in California. *Geomorphology* 31:265–90
- Janda RJ, Meyer DF, Childers D. 1984. Sedimentation and geomorphic changes during and following the 1980–1983 eruptions of Mount St. Helens, Washington. *Shin Sabo* 37(2):10–21 and 37(3):5–19
- Jefferson A, Grant GE, Lewis SL, Lancaster ST. 2010. Coevolution of hydrology and topography on a basalt landscape in the Oregon Cascade Range, USA. *Earth Surf. Process. Landf.* 35:803–16
- Jerolmack DJ, Mohrig D. 2007. Conditions for branching in depositional rivers. *Geology* 35:463–66
- Jitousono T, Shimokawa E, Teramoto Y, Nagata O. 1996. Distribution of ash fall deposit and infiltration rate on the flank of Unzen volcano. *J. Jpn. Soc. Eros. Control Eng.* 49(3):33–36 (in Japanese)
- Johnson AC, Wilcock P. 1998. Effect of root strength and soil saturation on hillslope stability in forests with natural cedar decline in headwater regions of SE Alaska. *Proc. Headwater '98, Fourth Int. Conf. Headwater Control, Merano, Italy*, pp. 381–87. Rotterdam, Neth.: Balkema
- Johnson MG, Beschta RL. 1980. Logging, infiltration capacity, and surface erodibility in western Oregon. *J. For.* 78:334–37
- Jones JA. 2000. Hydrologic processes and peak discharge response to forest removal, regrowth, and roads in 10 small experimental basins, western Cascades, Oregon. *Water Resour. Res.* 36:2621–42
- Kadomura H, Imagawa T, Yamamoto H. 1983. Eruption-induced rapid erosion and mass movements on Usu Volcano, Hokkaido. *Z. Geomorphol. Suppl.* 46:123–42
- Kataoka KS, Manville V, Nakajo T, Urabe A. 2009. Impacts of explosive volcanism on distal alluvial sedimentation—examples from the Pliocene–Holocene volcanoclastic successions of Japan. *Sediment. Geol.* 220:306–17
- Kelfoun K, Legros F, Gourgaud A. 2000. A statistical study of trees damaged by the 22 November 1994 eruption of Merapi volcano (Java, Indonesia): relationships between ash-cloud surges and block-and-ash flows. *J. Volcanol. Geotherm. Res.* 100:379–93
- Kesel RH, Lowe DR. 1987. Geomorphology and sedimentology of the Toro Amarillo alluvial fan in a humid tropical environment, Costa Rica. *Geogr. Ann. Ser. A* 69:85–99
- Kisa H, Yamakoshi T, Ishizuka T, Sugiyama M, Takiguchi S. 2013. The feature of surface runoff caused by rainfall on hillslopes covered with the tephra by the 2011 eruption of Shinmoe-dake, Kirishima volcano. *J. Jpn. Soc. Eros. Control Eng.* 65(6):12–21 (in Japanese, with English abstr.)
- Kuenzi WD, Horst OH, McGehee RV. 1979. Effect of volcanic activity on fluvial-deltaic sedimentation in a modern arc-trench gap, southwestern Guatemala. *GSA Bull.* 90:827–38
- Lavigne F. 2004. Rate of sediment yield following small-scale volcanic eruptions: a quantitative assessment at the Merapi and Semeru stratovolcanoes, Java, Indonesia. *Earth Surf. Process. Landf.* 29:1045–58
- Lavigne F, Suwa H. 2004. Contrasts between debris flows, hyperconcentrated flows and stream flows at a channel of Mount Semeru, East Java, Indonesia. *Geomorphology* 61:41–58
- Lavigne F, Thouret JC, Voight B, Suwa H, Sumaryono A. 2000. Lahars at Merapi volcano, Central Java: an overview. *J. Volcanol. Geotherm. Res.* 100:423–56
- Leavesley GH, Lusby GC, Lichty RW. 1989. Infiltration and erosion characteristics of selected tephra deposits from the 1980 eruption of Mount St. Helens, Washington, USA. *Hydrol. Sci. J.* 34(3):339–53
- Lettenmaier DP, Burges SJ. 1981. *Estimation of flood frequency changes in the Toutle and Cowlitz River basins following the eruption of Mt. St. Helens*. Charles W. Harris Hydraul. Lab. Tech. Rep. 69, Dep. Civ. Eng., Univ. Wash., Seattle. 73 pp.
- Lipman PW, Mullineaux DR, eds. 1981. *The 1980 Eruptions of Mount St. Helens, Washington*. USGS Prof. Pap. 1250. Washington, DC: USGS. 844 pp.
- Lisle T. 1995. Effects of coarse woody debris and its removal on a channel affected by the 1980 eruption of Mount St. Helens, Washington. *Water Resour. Res.* 31(7):1797–808

- Lisle TE, Cui Y, Parker G, Pizzuto JE, Dodd AM. 2001. The dominance of dispersion in the evolution of bed material waves in gravel-bed rivers. *Earth Surf. Process. Landf.* 26:1409–20
- Lombard RE, Miles MB, Nelson LM, Kresh DL, Carpenter PJ. 1981. The impact of mudflows of May 18 on the lower Toutle and Cowlitz Rivers. See Lipman & Mullineaux 1981, pp. 693–99
- Macías JL, Capra L, Scott KM, Espíndola JM, García-Palomo A, Costa JE. 2004. The 26 May 1982 breakout flows derived from failure of a volcanic dam at El Chichón, Chiapas, Mexico. *GSA Bull.* 116:233–46
- Major JJ. 2004. Posteruption suspended sediment transport at Mount St. Helens: decadal-scale relationships between landscape adjustments and river discharges. *J. Geophys. Res.* 109(F1):F01002
- Major JJ, Mark LE. 2006. Peak flow responses to landscape disturbances caused by the cataclysmic 1980 eruption of Mount St. Helens, Washington. *GSA Bull.* 118:938–58
- Major JJ, Pierson TC, Dinehart RL, Costa JE. 2000. Sediment yield following severe volcanic disturbance—a two-decade perspective from Mount St. Helens. *Geology* 28:819–22
- Major JJ, Pierson TC, Hoblitt RP, Moreno H. 2013. Pyroclastic density currents associated with the 2008–2009 eruption of Chaitén Volcano (Chile): forest disturbances, deposits, and dynamics. *Andean Geol.* 40(2):324–58
- Major JJ, Yamakoshi T. 2005. Decadal-scale change of infiltration characteristics of a tephra-mantled hillslope at Mount St. Helens, Washington. *Hydrol. Process.* 19:3621–30
- Manville V, Hodgson KA, Nairn IA. 2007. A review of break-out floods from volcanogenic lakes in New Zealand. *N.Z. J. Geol. Geophys.* 50:131–50
- Manville V, Németh K, Kano K. 2009a. Source to sink: a review of three decades of progress in understanding of volcanoclastic processes, deposits, and hazards. *Sediment. Geol.* 220:136–61
- Manville V, Segsneider B, Newton E, White JDL, Houghton BF, Wilson CJN. 2009b. Environmental impact of the 1.8 ka Taupo eruption, New Zealand: landscape responses to a large-scale explosive rhyolite eruption. *Sediment. Geol.* 220:318–36
- Manville V, Wilson CJN. 2004. The 26.5 ka Oruanui eruption, New Zealand: a review of the roles of volcanism and climate in the post-eruptive sedimentary response. *N.Z. J. Geol. Geophys.* 47:525–47
- McGuire WJ. 1996. Volcano instability: a review of contemporary themes. In *Volcano Instability on the Earth and Other Planets*, ed. WJ McGuire, AP Jones, J Neuberg, pp. 1–23. Geol. Soc. Lond. Spec. Publ. 110. London: Geol. Soc. Lond.
- Meyer DF, Martinson HA. 1989. Rates and processes of channel development and recovery following the 1980 eruption of Mount St. Helens, Washington. *Hydrol. Sci. J.* 34:115–27
- Miller DE, Gardner WH. 1962. Water infiltration into stratified soil. *Proc. Soil Sci. Soc. Am.* 26:115–19
- Mills MJ. 2000. Volcanic aerosol and global atmospheric effects. See Sigurdsson et al. 2000, pp. 931–43
- Miyabuchi Y, Shimizu A, Takeshita K. 1999. Grain size characteristics and infiltration rates of deposits associated with the 1990–95 eruption of Unzen volcano, Japan. *Trans. Jpn Geomorphol. Union* 30:85–96 (in Japanese, with English abstr.)
- Montgomery DR, Panfil MS, Hayes SK. 1999. Channel-bed mobility response to extreme sediment loading at Mount Pinatubo. *Geology* 27:271–74
- Nakada S, Shimizu H, Ohta K. 1999. Overview of the 1990–1995 eruption at Unzen Volcano. *J. Volcanol. Geotherm. Res.* 89:1–22
- Newhall CG, Punongbayan RS, eds. 1996. *Fire and Mud: Eruptions and Lahars of Mount Pinatubo, Philippines*. Seattle: Univ. Wash. Press. 1126 pp.
- Nicholas AP, Ashworth PJ, Kirkby MJ, Macklin MG, Murray T. 1995. Sediment slugs: large-scale fluctuations in fluvial sediment transport rates and storage volumes. *Prog. Phys. Geogr.* 19:500–19
- Nomura Y, Kosugi K, Mizuyama T. 2003. Physical properties of volcanic ash deposits in Miyakejima, Mt. Usu and Sakurajima: analysis of physical properties of ash deposits in relation to mudflow occurrences. *J. Jpn. Soc. Eros. Control Eng.* 55(6):3–12 (in Japanese, with English abstr.)
- Ogawa Y, Daimaru H, Shimizu A. 2007. Experimental study of post-eruption overland flow and sediment load from slopes overlain by pyroclastic-flow deposits, Unzen volcano, Japan. *Geomorphol. Relief Process. Environ.* 3:237–46
- Okuda S, Suwa H, Okunishi K, Nakano M, Yokoyama K. 1977. Synthetic observation on debris flow: Part 3. *Annu. Disaster Prev. Res. Inst. Kyoto Univ.* 20B(1):237–63

- Onda Y, Takenaka C, Mizuyama T. 1996. The mechanism inducing the infiltration rate lowering of Unzen volcanic ash. *J. Jpn. Soc. Eros. Control Eng.* 49(1):25–30 (in Japanese, with English abstr.)
- Orwig CE, Mathison JM. 1982. Forecasting considerations in Mount St. Helens affected rivers. *Proc. Mount St. Helens: Effects Water Resour., Oct. 7–8, 1981, Jantzen Beach, Or.*, pp. 272–92. Pullman, Wash.: Wash. State Water Res. Cent., Wash. State Univ.
- Pareschi MT, Favalli M, Giannini F, Sulpizio R, Zanchetta G, Santacroce R. 2000. May 5, 1998, debris flows in circum-Vesuvian areas (southern Italy): insights for hazard assessment. *Geology* 28:639–42
- Phillips JD. 2009. Changes, perturbations, and responses in geomorphic systems. *Prog. Phys. Geogr.* 33:17–30
- Piégay H, Schumm SA. 2003. System approaches in fluvial geomorphology. In *Tools in Fluvial Geomorphology*, ed. GM Kondolf, H Piégay, pp. 105–34. New York: Wiley
- Pierson TC. 2005. Hyperconcentrated flow—transitional process between water flow and debris flow. In *Debris-Flow Hazards and Related Phenomena*, ed. M Jakob, O Hungr, pp. 159–202. Chichester, UK: Springer-Praxis
- Pierson TC, Daag AS, Delos Reyes PJ, Regalado MTM, Solidum RU, Tubianosa BS. 1996. Flow and deposition of posteruption hot lahars on the east side of Mount Pinatubo, July–October 1991. See Newhall & Punongbayan 1996, pp. 921–50
- Pierson TC, Janda RJ, Thouret J-C, Borrero CA. 1990. Perturbation and melting of snow and ice by the 13 November 1985 eruption of Nevado del Ruiz, Colombia, and consequent mobilization, flow and deposition of lahars. *J. Volcanol. Geotherm. Res.* 41:17–66
- Pierson TC, Janda RJ, Umbal JV, Daag AS. 1992. *Immediate and long-term hazards from lahars and excess sedimentation in rivers draining Mt. Pinatubo, Philippines*. USGS Water-Res. Investig. Rep. 92-4039, US Dep. Inter., USGS, Cascades Volcano Obs., Vancouver, WA
- Pierson TC, Major JJ, Amigo Á, Moreno H. 2013. Acute sedimentation response to rainfall following the explosive phase of the 2008–2009 eruption of Chaitén volcano, Chile. *Bull. Volcanol.* 75(5):723
- Pierson TC, Pringle PT, Cameron KA. 2011. Magnitude and timing of downstream channel aggradation and degradation in response to a dome-building eruption at Mount Hood, Oregon. *GSA Bull.* 123:3–20
- Podolak CJP, Wilcock PR. 2013. Experimental study of the response of a gravel streambed to increased sediment supply. *Earth Surf. Process. Landf.* 38:1748–64
- Pringle P, Scott K. 2001. Postglacial influence of volcanism on the landscape and environmental history of the Puget Lowland, Washington: a review of geologic literature and recent discoveries, with emphasis on the landscape disturbances associated with lahars, lahar runouts, and associated flooding. *Proc. Puget Sound Res. Conf., 5th, Feb. 12–14, Bellevue, Wash.* Olympia, WA: Puget Sound Partnersh. http://archives.eopugetsound.org/conf/2001PS_ResearchConference/sessions/oral/4d_pring.pdf
- Procter J, Cronin SJ, Fuller IC, Lube G, Manville V. 2010. Quantifying the geomorphic impacts of a lake-breakout lahar, Mount Ruapehu, New Zealand. *Geology* 38:67–70
- Punongbayan RS, Newhall CG, Hoblitt RP. 1996. Photographic record of rapid geomorphic change at Mount Pinatubo, 1991–94. See Newhall & Punongbayan 1996, pp. 21–66
- Reid LM, Lewis J. 2009. Rates, timing, and mechanisms of rainfall interception loss in a coastal redwood forest. *J. Hydrol.* 375:459–70
- Roche O, Phillips JC, Kelfoun K. 2013. Pyroclastic density currents. In *Modeling Volcanic Processes: The Physics and Mathematics of Volcanism*, ed. SA Fagents, TKP Gregg, RMC Lopes, pp. 203–29. Cambridge, UK: Cambridge Univ. Press
- Rodolfo KS. 1989. Origin and early evolution of lahar channel at Mabinit, Mayon Volcano, Philippines. *GSA Bull.* 101:414–26
- Rodolfo KS, Umbal JV, Alonso RA, Remotigue CT, Paladio-Melosantos ML, et al. 1996. Two years of lahars on the western flank of Mount Pinatubo: initiation, flow processes, deposits, and attendant geomorphic and hydraulic changes. See Newhall & Punongbayan 1996, pp. 989–1013
- Roering JJ, Marshall J, Booth AM, Mort M, Jin Q. 2010. Evidence for biotic controls on topography and soil production. *Earth Planet. Sci. Lett.* 298:183–90
- Römkens MJM, Prasad SN, Whisler FD. 1990. Surface sealing and infiltration. In *Process Studies in Hillslope Hydrology*, ed. MG Anderson, TP Burt, pp. 127–72. Chichester, UK: Wiley

- Rosenfeld CL, Beach GL. 1983. *Evolution of a drainage network: remote sensing analysis of the North Fork Toutle River, Mount St. Helens, Washington*. Water Resour. Res. Inst. Rep. WRR1-88, Oreg. State Univ., Corvallis, OR. 100 pp.
- Rosgen DL. 1994. A classification of natural rivers. *Catena* 22:169–99
- Schneider A, Gerke HH, Maurer T, Nenov R. 2013. Initial hydro-geomorphic development and rill network evolution in an artificial catchment. *Earth Surf. Process. Landf.* 38:1496–512
- Schumm SA. 1985. Patterns of alluvial rivers. *Annu. Rev. Earth Planet. Sci.* 13:5–27
- Schumm SA, Rea DK. 1995. Sediment yield from disturbed earth systems. *Geology* 23:391–94
- Scott KM. 1988. Origin, behavior, and sedimentology of prehistoric catastrophic lahars at Mount St. Helens, Washington. In *Sedimentologic Consequences of Convulsive Geologic Events*, ed. HE Clifton, pp. 23–36. GSA Spec. Pap. 229. Boulder, CO: GSA
- Scott KM, Janda RJ, de la Cruz EG, Gabinete E, Eto I, et al. 1996. Channel and sedimentation responses to large volumes of 1991 volcanic deposits on the east flank of Mount Pinatubo. See Newhall & Punongbayan 1996, pp. 971–88
- Scott WE, Hoblitt RP, Torres RC, Self S, Martinez MML, Nillos T Jr. 1996. Pyroclastic flows of the June 5, 1991, climactic eruption of Mount Pinatubo. See Newhall & Punongbayan 1996, pp. 545–70
- Segerstrom K. 1950. Erosion studies at Parícutin, State of Michoacan, Mexico. *USGS Bull.* 965-A:1–164
- Segerstrom K. 1960. Erosion and related phenomena at Parícutin in 1957. *USGS Bull.* 1104-A:1–18
- Shimokawa E, Jitousono T. 1997. Field survey for debris flow in volcanic area. In *Recent Developments on Debris Flows*, ed. A Armanini, M Michiue, pp. 46–63. Lect. Notes Earth Sci. 64. Berlin/Heidelberg: Springer-Verlag
- Shimokawa E, Jitousono T, Tsuchiya S. 1996. Sediment yield from the 1984 pyroclastic flow deposit covered hillslopes in Merapi volcano, Indonesia. *J. Jpn. Soc. Eros. Control Eng.* 48(Spec. Issue):101–7
- Shimokawa E, Jitousono T, Yazawa A, Kawagoe R. 1989. An effect of tephra cover on erosion processes of hillslopes in and around Sakurajima Volcano. *Proc. Int. Symp. Eros. Volcan. Debris Flow Technol.*, July 31–Aug. 3, Yogyakarta, Indonesia, V32-1–V32-35. Yogyakarta, Indones.: Minist. Public Works
- Siebert L. 2002. Landslides resulting from structural failure of volcanoes. In *Catastrophic Landslides: Effects, Occurrence, and Mechanisms*, ed. SG Evans, JV DeGraff, pp. 209–35. GSA Rev. Eng. Geol. 15. Boulder, CO: GSA
- Sigurdsson H, Houghton BF, McNutt SR, Rymer H, Stix J, eds. 2000. *Encyclopedia of Volcanoes*. San Diego: Academic. 1,417 pp.
- Simon A. 1999. *Channel and drainage-basin response of the Toutle River system in the aftermath of the 1980 eruption of Mount St. Helens, Washington*. USGS Open-File Rep. 96-633, US Dep. Inter., USGS, Cascades Volcano Obs., Vancouver, WA. 130 pp.
- Smith GA. 1987. The influence of explosive volcanism on fluvial sedimentation: the Deschutes Formation (Neogene) in central Oregon. *J. Sediment. Petrol.* 57:613–29
- Smith GA. 1991. Facies sequences and geometries in continental volcanoclastic sequences. In *Sedimentation in Volcanic Settings*, ed. RV Fisher, GA Smith, pp. 109–21. SEPM Spec. Publ. 45. Tulsa, OK: Soc. Sediment. Geol.
- Smith RD, Swanson FJ. 1987. Sediment routing in a small drainage basin in the blast zone at Mount St. Helens, Washington, U.S.A. *Geomorphology* 1:1–13
- Suwa H, Sumaryono A. 1996. Sediment discharge by storm runoff from a creek on Merapi volcano. *J. Jpn. Soc. Eros. Control Eng.* 48:117–28
- Suwa H, Yamakoshi T. 1999. Sediment discharge by storm runoff at volcanic torrents affected by eruption. *Z. Geomorphol. Suppl.* 114:63–88
- Swanson FJ, Collins BD, Dunne T, Wicherski BP. 1983. Erosion of tephra from hillslopes near Mount St. Helens and other volcanoes. *Proc. Symp. Eros. Control Volcan. Areas, July 6–9, 1982, Seattle and Vancouver, Wash.*, pp. 183–221. Public Works Res. Inst. Tech. Memo. 1908. Tsukuba, Jpn.: Publ. Works Res. Inst.
- Swanson FJ, Janda RJ, Dunne T, Swanston DN, eds. 1982. *Sediment Budgets and Routing in Forested Drainage Basins*. USDA For. Serv. Gen. Tech. Rep. PNW-141. Washington, DC: US For. Serv. 165 pp.
- Swanson FJ, Jones JA, Crisafulli CM, Lara A. 2013. Effects of volcanic and hydrologic processes on forest vegetation: Chaitén Volcano, Chile. *Andean Geol.* 40(2):359–91

- Swanson FJ, Major JJ. 2005. Physical events, environments, and geological-ecological interactions at Mount St. Helens: March 1980–2004. See Dale et al. 2005, pp. 27–44
- Tagata S, Yamakoshi T, Doi Y, Kurihara J, Terada H, Sakai N. 2006. Post-eruption characteristics of rainfall runoff and sediment discharge at the Miyakejima Volcano, Japan. *Proc. INTERPRAEVENT Int. Symp., Sept. 26, Nigata, Jpn.*, pp. 291–301. Tokyo: Univers. Acad. Press
- Takehita K. 1987. Influence of change in soil infiltration due to large-scale tephra cover on erosion processes of mountains. *Trans. Jpn. Geomorphol. Union* 8:227–48 (in Japanese, with English abstr.)
- Teramoto Y, Shimokawa E, Jitousono T. 2006. Effects of volcanic ash on the runoff process in Sakurajima volcano. *Proc. INTERPRAEVENT Int. Symp., Sept. 26, Nigata, Jpn.*, pp. 303–10. Tokyo: Univers. Acad. Press
- Thorn CE, Welford MR. 1994. The equilibrium concept in geomorphology. *Ann. Assoc. Am. Geogr.* 84:666–96
- Tindall JA, Kunkel JR. 1999. *Unsaturated Zone Hydrology for Scientists and Engineers*. Upper Saddle River, NJ: Prentice Hall. 624 pp. 1st ed.
- Todesco M, Todini E. 2004. Volcanic eruption induced floods: a rainfall-runoff model applied to the Vesuvian region (Italy). *Nat. Hazards* 33:223–45
- Umbal JV. 1997. Five years of lahars at Pinatubo Volcano: declining but still potentially lethal hazards. *J. Geol. Soc. Philipp.* 52(1):1–19
- Umbal JV, Rodolfo KS. 1996. The 1991 lahars of southwestern Mount Pinatubo and evolution of the lahar-dammed Mapanuepe Lake. See Newhall & Punongbayan 1996, pp. 951–70
- Vallance JW. 2000. Lahars. See Sigurdsson et al. 2000, pp. 601–16
- Vallance JW. 2005. Volcanic debris flows. In *Debris-Flow Hazards and Related Phenomena*, ed. M Jakob, O Hungr, pp. 247–74. Chichester, UK: Springer-Praxis
- Vallance JW, Scott KM. 1997. The Osceola Mudflow from Mount Rainier: sedimentology and hazard implications of a huge clay-rich debris flow. *GSA Bull.* 109:143–63
- Voight B, Glicken H, Janda RJ, Douglass PM. 1981. Catastrophic rockslide avalanche of May 18. See Lipman & Mullineaux 1981, pp. 347–77
- Waldron HH. 1967. Debris flow and erosion control problems caused by the ash eruptions of Irazú Volcano, Costa Rica. *USGS Bull.* 1241-I:1–37
- Waythomas CF, Scott WE, Nye JC. 2010. The geomorphology of an Aleutian volcano following a major eruption: the 7–8 August 2008 eruption of Kasatochi Volcano, Alaska, and its aftermath. *Arct. Antarct. Alp. Res.* 42:260–75
- White JDL, Houghton BF. 2006. Primary volcanoclastic rocks. *Geology* 34:677–80
- White JDL, Houghton BF, Hodgson KA, Wilson CJN. 1997. Delayed sedimentary response to the A.D. 1886 eruption of Tarawera, New Zealand. *Geology* 25:459–62
- Wilcock PR, Crowe JC. 2003. Surface-based transport model for mixed-size sediment. *J. Hydraul. Eng.* 129:120–28
- Willingham WF. 2005. The Army Corps of Engineers' short-term response to the eruption of Mount St. Helens. *Or. Hist. Q.* 106:174–203
- Wilson CJN. 1985. The Taupo eruption, New Zealand: II. The Taupo ignimbrite. *Philos. Trans. R. Soc. A* 314:229–310
- Wilson CJN, Houghton BF. 2000. Pyroclast transport and deposition. See Sigurdsson et al. 2000, pp. 545–54
- Wohl E. 2013. Floodplains and wood. *Earth-Sci. Rev.* 123:194–212
- Wu BS, Zheng S, Thorne CR. 2012. A general framework for using the rate law to simulate morphological response to disturbance in the fluvial system. *Prog. Phys. Geogr.* 36(5):575–97
- Yamakoshi T, Doi Y, Osanai N. 2005. Post-eruption hydrology and sediment discharge at the Miyakejima volcano, Japan. *Z. Geomorphol. Suppl.* 140:55–72
- Yamakoshi T, Ishida T, Nakano M, Yamada T. 2002. Characteristics of sediment movement phenomena caused by rainfall after the 2000 eruption of Usu volcano. *Proc. INTERPRAEVENT 2002 Pac. Rim Int. Congr., Oct. 14–18, Matsumoto, Jpn.*, 1:145–51. Klagenfurt, Austria: INTERPRAEVENT
- Yamakoshi T, Sasahara K, Tagata S, Ishida T, Takeshima H, Wakabayashi E. 2006. The surface runoff prediction model for the fine-tephra mantled slope. *J. Jpn. Soc. Eros. Control Eng.* 59(4):24–31 (in Japanese, with English abstr.)

- Yamakoshi T, Suwa H. 2000. Post-eruption characteristics of surface runoff and sediment discharge on the slopes of pyroclastic-flow deposits, Mount Unzen, Japan. *Trans. Jpn. Geomorphol. Union* 21(4):469–97
- Yamamoto H. 1984. Erosion of the 1977–1978 tephra layers on a slope of Usu Volcano, Japan. *Trans. Jpn. Geomorphol. Union* 5:111–24 (in Japanese, with English abstr.)
- Yamamoto H, Imagawa T. 1983. Surface runoff on a slope covered by 1977–1978 tephra from Usu Volcano. *Hydrology* 13:25–33 (in Japanese, with English abstr.)
- Yamamoto H, Kadomura H, Suzuki R, Imagawa T. 1980. Mudflows from a 1977–1978 tephra-covered watershed on Usu Volcano, Hokkaido, Japan. *Trans. Jpn. Geomorphol. Union* 1:73–88 (in Japanese, with English abstr.)
- Zheng S, Wu B, Thorne CR, Simon A. 2014. Morphological evolution of the North Fork Toutle River following the eruption of Mount St. Helens, Washington. *Geomorphology* 208:102–16
- Ziemer RR. 1981. Roots and the stability of forested slopes. In *Erosion and Sediment Transport in Pacific Rim Steeplands*, ed. TRH Davies, AJ Pearce, pp. 343–61. Int. Assoc. Hydrol. Sci. Publ. 132. Wallingford, UK: IAHS